Geology of the Lindenow Fjord – Kangerluluk area, South-East Greenland: preliminary results of Suprasyd 1994

Cees Swager, Brian Chadwick, Tom Frisch,
Adam Garde, Hans Kristian Schønwandt,
Henrik Stendal and Bjørn Thomassen

Open File Series 95/6

August 1995

GGU

GRØNLANDS GEOLOGISKE UNDERSØGELSE
Ujarassiortut Kalaallit Nunaanni Misissuisoqarfiat
GEOLOGICAL SURVEY OF GREENLAND

GRØNLANDS GEOLOGISKE UNDERSØGELSE
Ujarassiortut Kalaallit Nunaanni Misissuisoqarfiat
GEOLOGICAL SURVEY OF GREENLAND
Øster Voldgade 10, DK-1350 Copenhagen K, Denmark

The Geological Survey of Greenland (GGU) is a research institute affiliated to the Mineral Resources Administration for Greenland (MRA) within the Danish Ministry of Environment and Energy. As with all other activities involving mineral resources in Greenland, GGU's investigations are carried out within the framework of the policies decided jointly by the Greenland Home Rule Authority and the Danish State.

Open File Series

The Open File Series consists of unedited reports and maps that are made available quickly in limited numbers to the public. They are a non-permanent form of publication that may be cited as sources of information. Certain reports may be replaced later by edited versions.

Citation form

Open File Series Grønlands Geologiske Undersøgelse

conveniently abbreviated to:

Open File Ser. Grønlands geol. Unders.

GGU's Open File Series består af uredigerede rapporter og kort, som publiceres hurtigt og i et begrænset antal. Disse publikationer er midlertidige og kan anvendes som kildemateriale. Visse af rapporterne vil evt. senere blive erstattet af redigerede udgaver.

ISSN 0903-7322

GRØNLANDS GEOLOGISKE UNDERSØGELSE

Open File Series 95/6

Geology of the Lindenow Fjord - Kangerluluk area, South-East Greenland: preliminary results of Suprasyd 1994

Cees Swager, Brian Chadwick, Tom Frisch, Adam Garde, Hans Kristian Schønwandt, Henrik Stendal and Bjørn Thomassen

August 1995

ABSTRACT

The Lindenow Fjord - Kangerluluk area in the southern part of South-East Greenland covers part of the early Proterozoic (*c.* 1.85-1.75 Ga) Ketilidian orogen. The map sheet area is underlain in the northwest by granodiorite s.l. of the Julianehåb batholith, and in the central and southeastern parts by supracrustal rocks consisting of migmatized metasediments (psammite, pelite, incl. turbiditic sequences, minor conglomerate), subordinate mafic metavolcanic rocks (basalt-andesite, hyaloclastite, agglomeratic and tuffaceous rocks; with interleaved mafic greywacke), and graphitic schist horizons. Mafic and ultramafic dykes ('appinites') occur throughout the sequence. Leucocratic autochthonous granite is common in larger volumes towards the east. Late stage rapakivi plutons (quartz monzonite, norite) intrude both the batholith and the supracrustal sequence. Granodiorite s.l. of the Julianehåb batholith contains a regional 060-trending foliation with local oblique sinistral and dextral shears, and was emplaced during sinistral transpression (Chadwick *et al.*, 1994). Main boundaries between batholith and supracrustal rocks are vertical 060-trending mylonitic shear zones, but variably dipping intrusive and possible unconformable contacts are observed.

Supracrustal rocks record more complex deformation including early isoclinal-recumbent folds (overturned sequences), south-vergent recumbent folds and E to ENE-trending upright folds. All fold styles are associated with migmatization and neosome veins in axial planar orientation. Local late stage microfolds appear not to have influenced regional geometry. Batholith type granodiorite was emplaced into the supracrustal sequence during ENE-trending folding.

Regional low P metamorphism in the supracrustal rocks increases from lower amphibolite facies (epidote amphibolite) in a narrow zone along the batholith boundary to upper amphibolite facies throughout the remainder. Granulite facies rocks lie to the south of the map sheet. Preliminary observations in pelitic rocks indicate a very early high T peak metamorphic assemblage and a second lower T metamorphic event late during and/or after ENE-trending folding, possibly coincident with rapakivi emplacement.

Both batholith and supracrustal rocks are part of U and Au geochemical provinces. The migmatitic supracrustal sequence is also characterized by elevated As and Sb. Stratabound mineralization of the 'graphite-Fe sulphide-chemical sediment-amphibolite' association include 'pelitic graphitic shale', 'metalliferous black shale' and mafic volcanic-

dominated end-members. All these are characterized by variably elevated Au and As. Epigenetic Au-Cu mineralization is noted in small veins in metabasalt and in small and large shear zones along the batholith - supracrustal boundary zone. Uranium mineralization, including the Illorsuit prospect, in migmatitic psammitic gneiss was remobilized during regional metamorphism and deformation.

CONTENTS

List of figures

List of tables

Map enclosures

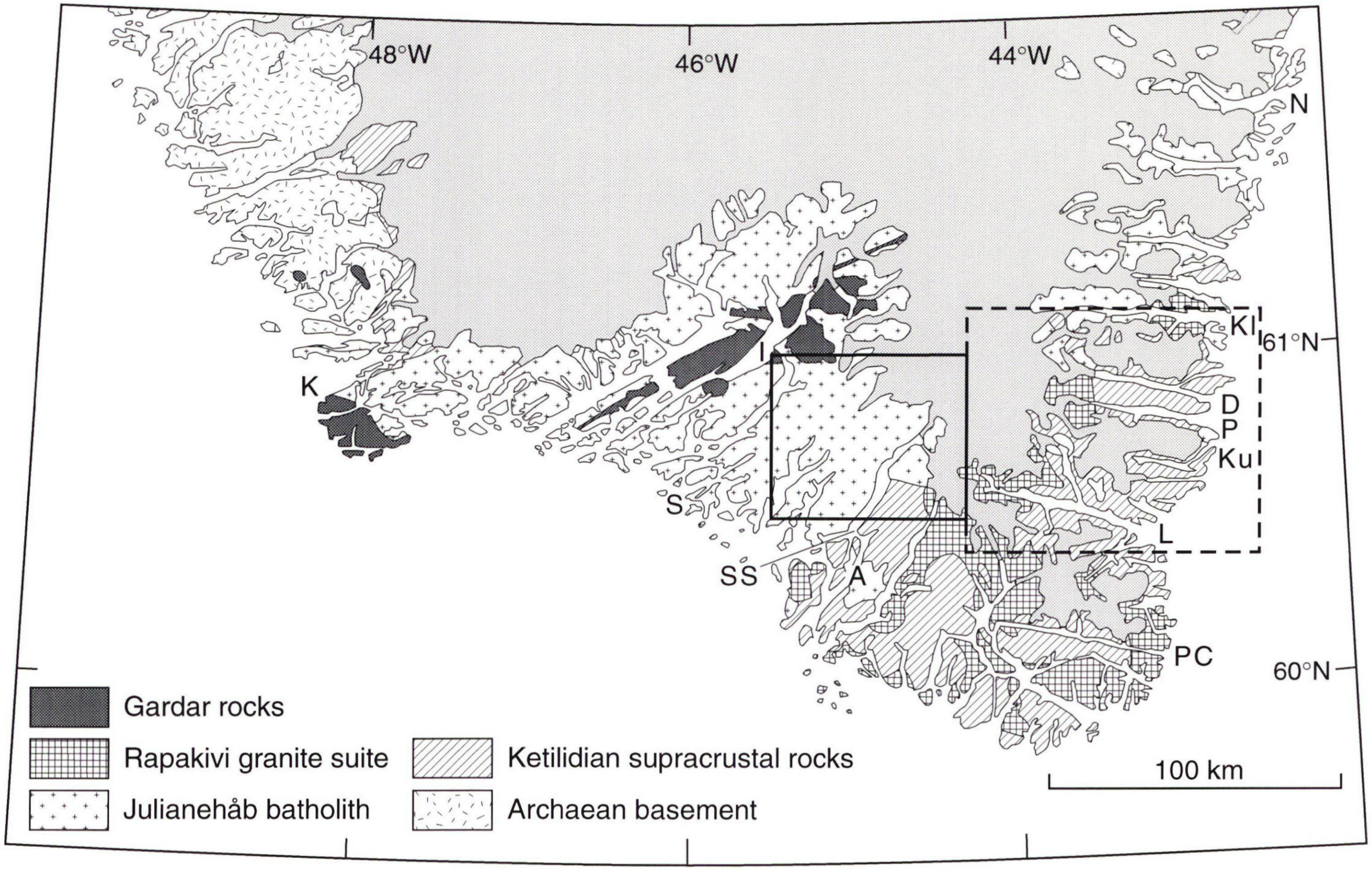

Figure 1. Geological sketch map of South Greenland with the position of the Søndre Sermilik 1:100 000 map sheet (solid outline) and the area described in this open file report (broken line) covering the Lindenow Fjord 1:100 000 map sheet and some additional areas to the north and south. A: Amitsoq, D: Danell Fjord, I: Igaliko Fjord, K: Kobberminebugt, Kl: Kangerluluk, Ku: Kutseq, L: Lindenow Fjord, N: Napasorsuaq Fjord, P: Paatussoq, PC: Prins Christian Sund, S: Saarloq, SS: Søndre Sermilik.

INTRODUCTION

The SUPRASYD project was initiated in 1992 to assess the geology, tectonic setting and mineral potential of the Lower Proterozoic Ketilidian orogenic belt, and in particular its supracrustal sequence, in South Greenland. During the first three field seasons work was concentrated on respectively a regional reconnaissance (geology, geochemistry) along the east coast (Nielsen *et al.*, 1993), mapping of part of the Julianehåb batholith and its mineralized shear zones on the west coast (Garde & Schønwandt, 1994), and regional mapping and investigations of documented alteration zones on both east and west coast of South Greenland (Garde & Schønwandt, in press).

Early results of the project have so far been published in GGU Open File Series and Reports. Some important contributions include a reassessment of presumed felsic volcanic rocks in the northern border zone along the east coast (Chadwick *et al.*, 1994a), a reappraisal of the structures and structural setting of the Julianehåb batholith (Chadwick *et al.*, 1994b), and the confirmation of the orogen as a gold and uranium metallogenic province and recognition of potential mineralized structures (Steenfelt *et al.*, 1992; Schønwandt, 1994). The new interpretation of the Julianehåb batholith forms the basis for a new plate tectonic model for the Ketilidian orogenic belt (Chadwick & Garde, in press). Detailed U-Pb zircon geochronology is an important part of the geological/metallogenic reassessment (M. Hamilton *et al.*, unpubl. 1995). Another product of the project will be the 1:100 000 Søndre Sermilik map sheet 60V3N and accompanying map sheet description, which are currently being prepared for publication.

The aim of this open file report is to present preliminary results of the geological and geochemical mapping between Kangerluluk and Lindenow Fjord on the east coast of South Greenland, an area directly to the east of the Søndre Sermilik map sheet. The area is largely underlain by high grade, migmatitic supracrustal rocks, intruded by large plutons of the rapakivi suite; in the northwest it contains parts of the Julianehåb batholith. The preliminary map compilation (enclosed Map 1: Preliminary Geological Map at 1:100 000) is based on the more systematic work in 1994 following the reconnaissance survey in 1992. Geochemical sampling in 1994 included 145 rock samples, 10 stream sediment samples and 10 panned heavy mineral concentrates (see enclosed Map 2: Geochemical Sample Map). All samples were analysed for 48 elements (see Tables 1-3).

Mapping of the Lindenow Fjord map sheet is planned to be completed during the 1996 field season. A major regional aeromagnetic survey covering a large part of the Ketilidian orogen, is planned for the summer of 1995, and is financed by the Greenland Home Rule Authority. In 1994 an off-shore seismic profile was recorded across the boundary of the Ketilidian with the Archaean craton to the north (T. Dahl-Jensen and Danish Lithosphere Centre, personal communication 1995).

REGIONAL SETTING

The Early Proterozoic Ketilidian mobile belt was originally divided into four zones (Allaart, 1976; see also Kalsbeek *et al.*, 1990), from northwest to southeast: 1. a northern border zone, where Ketilidian sedimentary and volcanic rocks overlie unconformably and with tectonic contacts the Archaean basement, 2. the granite zone, more recently renamed the Julianehåb batholith, consisting of variably deformed granites of calc-alkaline affinity, originally thought to consist of 'early' and 'late' phases, and apparently emplaced over a considerable period (*c.* 1850-1750 Ma; van Breemen *et al.*, 1974), 3. the folded migmatite zone with metasedimentary sequences and some mafic metavolcanics, and 4. the flat-lying migmatite zone.

The migmatitic supracrustal rocks are intruded by large plutons of the late tectonic rapakivi suite (quartz monzonite, norite) dated at 1755 Ma and 1740 Ma (Gulson & Krogh, 1975). The age of the amphibolite to granulite facies metamorphism of the supracrustal sequence was interpreted by Gulson & Krogh (1975) as *c.* 1800 Ma, i.e. the age of migmatite-granite veins which were presumed to be contemporaneous with the main metamorphic event. However, Dempster *et al.* (1991) suggested that peak metamorphic conditions were reached later during rapakivi suite emplacement. The metamorphic facies is characterized by low P - high T, with assemblages in the granulite domain implying very high thermal gradients (Dempster *et al.*, 1991).

Isotopic signatures indicate that the batholith and the supracrustal rocks contain predominantly Proterozoic crustal material, with only 10-15% contribution of Archaean crust (Patchett & Bridgewater, 1984). Hence the Ketilidian consists of juvenile, early Proterozoic crust, which is interpreted as an Andean-type magmatic arc, accreted onto the

Archaean craton (e.g. van Breemen *et al.*, 1974; Patchett & Bridgwater, 1984; Kalsbeek & Taylor, 1985; Kalsbeek, 1994; Chadwick & Garde, in press).

The border zone on the west coast contains sedimentary and mafic volcanic rocks that become progressively more deformed and metamorphosed towards the contact (Kobberminebugt shear zone) with the Julianahåb batholith. Close to the contact the supracrustal rocks are intruded by Ketilidian granites in which isotopic studies have detected major components of Archaean crustal material. No independent ages have been reported for the supracrustal rocks although they are generally regarded as Ketilidian in age. An extensive literature about the supracrustal rocks in the border zone has recently been summarized by Kalsbeek *et al.* (1990). Along the east coast Andrews *et al.* (1973) reported possible Ketilidian acid volcanic rocks and related gneisses, which were considered as favourable host rocks for massive sulphide mineralization. These rocks were subsequently dated as Archaean in age (Pedersen *et al.*, 1974). Furthermore, Chadwick *et al.* (1994a) who re-examined the type locality on Ikermit island, demonstrated that the sequence consists entirely of orthogneisses and common, narrow mylonite zones.

Tectonic models

Recently, more detailed interpretations of the tectonic setting of the Ketilidian orogenic belt have been published. Windley (1991), referring to the 1960s GGU mapping programme, proposed a plate tectonic model for the Ketilidian and compared it with the Himalayas. The Julianehåb batholith was interpreted to intrude an Andean-type continental margin of earlier accreted island arc volcanic and plutonic rocks. The border zone is a partly inverted back arc basin developed on the Archaean craton. The migmatitic paragneisses were interpreted as a sequence thickened by thrusting, as inferred from the early recumbent fold and nappe structures described by Escher (1966) and Dawes (1970). According to Windley (1991), this stacked pile subsequently collapsed, and rapakivi suite granites were emplaced in an extensional regime.

Brown *et al.* (1992) who worked only in the flat-lying migmatite zone, found that the metamorphic, structural and igneous history does not support Windley's (1991) model. Brown *et al.* pointed out that there are (no relics of) high-pressure metamorphic assemblages as would be expected in a stacked sequence, that there is little evidence for regional folding (apart from isolated recumbent folds), and that the bimodal nature of the rapakivi suite (quartz monzonite - norite) is not explained. Instead Brown *et al.* (1992) suggest that the juvenile Ketilidian crust was underplated by mafic magma (norite) during a regime of strong regional extension. This regime can explain the high T - low P metamorphism of the supracrustal sequence, and the energy for the crustal melting to form the quartz monzonite plutons. These were emplaced, possibly as sheets, along the ramps and flats of low angle ductile shear zones (Hutton *et al.*, 1990). Brown and co-workers proposed as a possible tectonic setting for this scenario a back arc environment, presumably behind the arc represented by the Julianehåb batholith. This model seems to require south or south-east dipping subduction below the batholith.

Recent fieldwork in the Søndre Sermilik map sheet area has led to a re-interpretation of the Julianehåb batholith (Chadwick *et al.*, 1994b). This reassessment has shown that the batholith is made up only of variably deformed granitic to dioritic plutonic rocks, and does not contain either 'older' gneiss or supracrustal remnants. Foliation, lineation and asymmetric fabrics led these authors to suggest that the batholith was emplaced in a sinistral transpressional regime.

Chadwick & Garde (in press) presented a tectonic model in which the Julianehåb batholith is the root of a magmatic/volcanic arc that shed its detritus to the southeast into a fore-arc with 'proximal psammite' and 'distal pelite' zones. These broadly correspond to the folded and flat-lying migmatite zones of Allaart (1976) respectively. The batholith was emplaced under a sinistral transpressional regime caused by oblique subduction of an oceanic plate underneath the Archaean craton to the northwest. Chadwick & Garde (in press) explained the high T metamorphism of the migmatitic supracrustal sequence in terms of mafic underplating, in a similar manner to that proposed by Brown *et al.* (1992). However, the Chadwick & Garde model requires underplating underneath the fore arc, rather than underneath an extensional back arc as envisaged by Brown *et al.* (1992). This overview of recent models suggests that in particular the relationship between the Julianehåb batholith and the high T - low P supracrustal sequence is not yet fully explained.

Regional stratigraphy

The supracrustal sequence exposed in the Lindenow Fjord map sheet area lies along strike of the Nanortalik, Tasiussaq and NE Tasermiut areas along the west coast of South

Greenland, mapped and described by Escher (1966), Dawes (1970) and Wallis (1966) respectively. Escher and Dawes recognized a (very) high grade (semi-)pelitic to psammitic complex with thin calc-silicate, graphitic sulphide-bearing, and amphibolitic layers, probably overlain by less deformed and/or less migmatitic meta-arkoses, with polymictic conglomerates, and mafic meta-volcanics. Wallis (1966) recognized the same rock types, dominated by psammitic/arkosic gneiss, with a possible central unit of semi-pelitic and pelitic gneiss.

Similar lithologies are present in the Lindenow Fjord map sheet area. A distinct stratigraphy with regional marker beds is not yet established. Psammitic gneiss is the dominant rock type, and has interleaved semi-pelitic schist or gneiss, and local marker beds defined by diopsidic psammite, amphibolitic meta-volcanic rocks or graphite - Fe-sulphide layers. In the Danell Fjord area psammites are overlain by semi-pelite to pelite, which includes turbidite-like sequences with perfectly preserved graded beds. A substantial, little deformed metabasalt sequence - with hyaloclastites, mafic tuffaceous beds and mafic greywackes as well as interbedded psammite and conglomerate - has been mapped along the contact zone between the Julianehåb batholith and the supracrustal sequence in the Sorte Nunatak - eastern Kangerluluk area. Its exact stratigraphic position in the metasedimentary sequence is not known, partly because of the many shear zones in the contact zone.

Another similarity with the west coast is the increase in metamorphic grade from rocks near the batholith to those further south or south-east. On a regional scale the metamorphic grade increases from north-west (amphibolite facies) to south-east (granulite facies; Wallis, 1966). Escher (1966) and Dawes (1970) contemplated a possible break between a lower, high grade gneiss and overlying, less deformed supracrustal rocks.

LITHOLOGY - SUPRACRUSTAL ROCKS

Psammitic rocks

Psammite is the major supracrustal lithology on the map sheet, and can be described in three groups on the basis of increasing volumes of migmatite and pegmatite, and a fourth group representing a calc-silicate (or diopsidic) facies.

Psammitic gneiss is light grey quartz-feldspar gneiss with small amounts of biotite, characterized by preserved primary layering. Thin pegmatite veins lie along bedding or early foliation planes, and initial recrystallization - migmatization (10-20%) has resulted in grain coarsening, growth of hornblende and local destruction of layering/bedding. In several areas cross bedding, trough and channel structures suggest shallow water deposition and provide reliable way-up criteria. North of central Danell Fjord a possible larger scale unconformity observed within a psammmitic sequence, separates migmatitic rocks from overlying finely bedded diopsidic facies rocks.

In migmatitic psammitic gneiss multiple generations of pegmatite veins and extensive migmatization have destroyed much of the detail of the original fine bedding, even though the overall layering is still preserved. In many areas migmatitic and finely bedded gneiss are interleaved on various scales; the migmatitic lithology is generally dominant. In places, at least three generations of pegmatite veins can be distinguished - sometimes emplaced along both layering and fold axial planes. Similar pegmatite 'histories' have been documented in more detail along the west coast (Dawes, 1965, 1970; Wallis, 1966). Highly migmatitic psammitic gneiss contains numerous and large pegmatite veins and aggregates, dykes and larger bodies of autochthonous (S-type) granite. There are gradations on various scales from preserved ghost layering to massive, leucocratic, very irregular feldspar-porphyritic granite with relics of partially digested layered gneiss. Agmatitic structures, chaotic folding or rotation of isolated gneissic blocks, and total dismemberment of amphibolite dykes are characteristic features. Pegmatite veins may contain some cordierite, garnet and/or magnetite, they commonly include coarse black tourmaline, and at one locality dumortierite was found.

The calc-silicate or diopsidic psammite facies contains originally calcareous layers, now occurring as thin packages (from few centimetres up to several metres) of usually well-bedded psammite with various, strictly bedding-controlled, proportions of diopside, or as quite substantial packages (several tens of metres) that include garnet-bearing and massive carbonate layers. The layers commonly show fine scale (over centimetres) zoning from the centre of the calcareous layer outwards - carbonate, garnet, diopside, locally tremolite, (hornblende) - suggesting local-scale metasomatic interaction with adjacent arkosic layers. In most instances the calc-silicate layers have preserved their internal coherence as intercalated psammite beds were migmatized. North of Lindenow Fjord, ovoid calc-silicate pods or 'concretions' occur parallel to the layering in psammitic gneiss, and commonly show distinct mineral zoning.

Pelitic and semi-pelitic rocks

Pelitic and semi-pelitic rocks are described in two main groups (i.e. schist and gneiss) that largely reflect increasing metamorphic grade and migmatization. Pelitic to semi-pelitic schist contains fine-grained, micaceous, slaty rocks interleaved with fine- to medium-grained psammitic/arkosic layers. In several areas turbidite-like sequences with regular graded-bedding are preserved. Andalusite is a common porphyroblast in a biotite-muscovite-quartz-feldspar matrix. Small quartz veins, in various generations and variously deformed, are common in these folded rocks. The metamorphic grade is lower amphibolite facies.

Pelitic (to semi-pelitic) gneiss is medium- to locally coarse-grained, commonly garnetiferous biotite-quartz-feldspar rocks, interleaved with more or less preserved psammitic layers. Reversal of the original sedimentary grain size distribution has occurred in these rocks because fine slaty layers have been converted into much coarser grained gneiss. Along the south coast of Danell Fjord the size and total volume of pegmatite appears to increase to the east, i.e. possibly corresponding with increasing metamorphic grade. Early small, garnetiferous, pegmatites are followed by progressively coarser and more leucocratic sills and dykes. The biotite-rich gneiss contains small fibrolitic sillimanite aggregates parallel to the main foliation or layering. Locally such aggregates occur as distinctive, whitish coloured 'fragments' clearly visible in hand specimen. Porphyroblasts include garnet, cordierite, as well as andalusite and K-feldspar. Unoriented muscovite porphyroblasts have formed in many micaceous layers. The sillimanite-biotite assemblage with extensive partial melting indicates upper amphibolite facies metamorphic conditions.

Graphitic schist association

Deep red-brown weathered graphitic and sulphidic schist layers, commonly associated with subordinate amphibolite, up to some 25 metres thick and persistent over kilometres, occur both within psammitic - pelitic and mafic volcanic sequences. Typically these associations contain chemical sedimentary layers including quartz-rich or chert bands. Both pyrrhotite and pyrite can be the main sulphide phase (from a few per cent to some 30%), accompanied by local chalcopyrite, sphalerite and arsenopyrite. Several types of occurrence of these graphitic layers can be distinguished on the basis of host rock association and geochemical signature (see section on Mineralization systems). Pelitic - graphitic schists occur throughout the supracrustal sequence, but at Stendalen a prominent gossanous graphitic schist layer shows elevated values for a wide range of elements, comparable to those in a 'metalliferous black shale' association. Graphitic layers, with or without chemical sediments or mafic volcaniclastic layers, also occur within mafic (Kutseq, Kangerluk) and ultramafic (Illukulik) volcanic rocks.

This general 'graphite - Fe-sulphide - chemical sediment - amphibolite' association probably formed in periods of reduced clastic supply, with chemical sediment and Fe sulphide indicating some exhalative activity. Quartz veining is extensive in graphitic and siliceous schist.

Conglomerate and breccia

Coarse polymict conglomerate was found north and south of Kangerluluk within cross-bedded psammitic gneiss, adjacent to the Graah Fjelde rapakivi intrusion. These conglomerates are similar to those described by Chadwick & Garde (in press) for the psammite zone close to the boundary with the Julianehåb batholith on the west coast. Clasts include grey amphibolite (possibly andesitic in origin), aplite and psammite; they are well-rounded, both matrix- and clast-supported, and distinctly linear. The conglomerates commonly lie at the base of graded units up to 40 cm thick.

Another variety of conglomerate mapped by Chadwick (1994) in the nunataks south of inner Kutseq is characterized by abundant, rounded clasts of vein quartz and additional psammite, possible felsic volcanic, aplite and grey granite clasts. These clasts, with a marked elongation parallel to the regional 060-trending lineation, are poorly sorted, clast- or matrix-supported, and have a calcareous matrix inferred from coarse diopside and garnet pods and cavities. Large scale trough cross-bedding within the coarse conglomeratic section of the sequence indicates a fluviatile or beach environment. Interleaved psammite with smaller scale cross-bedding suggests a braided river or shallow marine setting. The well-preserved primary structures demonstrate that this very gently dipping conglomerate sequence is overturned, implying the presence of a regional scale nappe.

Other conglomerate and breccia layers have been found, for example in the Sorte Nunatak - Kangerluluk mafic meta-volcanic sequence. Many of these conglomerates and breccias contain predominantly intermediate to mafic clasts, although some psammite or granite/aplite clasts are observed. However, south of eastern Patussoq a similar breccia occurs within a thick psammitic - pelitic gneiss sequence. This bedded breccia is dominated by clasts of feldspar-phyric amphibolite with hornblende prisms, with some psammite and aplite clasts, within a biotite amphibolitic matrix. The clasts are unsorted, mostly angular and strongly lineated parallel to the regional shallow ENE-plunging mineral lineation/fold axis.

Mafic volcanic rocks: metabasalt - hyaloclastite - agglomerate

Mafic volcanic and volcaniclastic rocks occur as thin (10-100m) discontinuous amphibolite layers within the meta-sedimentary gneisses, and as thicker (>200m) sequences of well-preserved, low strain metabasalt, hyaloclastite, agglomerate and associated volcaniclastic rocks. A prominent, gently dipping metabasalt - hyaloclastite sequence in the Sorte Nunatak - Kangerluluk area is intruded by granite of the Julianehåb batholith, although Chadwick & Garde (in press) also suggest a local unconformity between granite and overlying supracrustal rocks. At Sorte Nunatak a detailed stratigraphy for this sequence is impossible to establish because of inaccessibility. Both undeformed basalt with amygdales, plagioclase and/or augite phenocrysts, and olivine-bearing mafic inclusions and slightly deformed, epidotized varieties have been sampled on glaciers below vertical outcrops. The volcanic rocks are interlayered with mafic greywackes which show cross bedding, large scale trough or channel structures, and polymict conglomerates with granite, psammite and basalt pebbles. Observations from the air, to the north of Sorte Nunatak itself, noted substantial conglomerate between the metavolcanic sequence and underlying granite.

On the plateau south of central Kangerluluk spectacular basalt hyaloclastites, agglomerates and finely bedded tuffaceous and reworked volcaniclastic sequences with indications for soft sediment deformation including slump folds and dewatering structures are interlayered with andesitic to basaltic flows (Chadwick, 1994). These epidote-altered rocks, which record low amphibolite facies (or epidote amphibolite) metamorphic conditions and low strain, are shown on the map as a single package with the Sorte Nunatak sequence.

Mafic volcanic rocks: amphibolite

Amphibolite includes recrystallized layers, although in many occurrences primary structures can still be recognized, at least locally, such as pillowed flows (e.g. south of Kutseq), finely bedded tuffaceous, agglomeratic and reworked volcaniclastic beds, and local layers of polymictic conglomerate with some felsic pebbles. In more strongly deformed domains hornblende-quartz-feldspar to massive hornblende schist is sometimes garnetiferous. Geochemical analysis has confirmed the presence of 'ultramafic amphibolite' (43-47% SiO2, MgO *c.* 20%) east of Illukulik along the north shore of Lindenow Fjord, probably below the Stendalen graphitic-sulphidic schist layer, and as enclaves within rapakivi granite at Illorsuit. All three occurrences may represent the same stratigraphic layer.

Many amphibolite occurrences, including the smallest lenses, are associated with fine pelitic, locally graphitic, schist. Biotite is a common metamorphic product, present in high concentrations along contacts with the metasedimentary rocks. These biotite-rich contact zones stand out because of their rusty-brown weathering. Calc-silicates (diopside, garnet) alteration along veins, pillow rims or in irregular patches are relatively common. Pyrrhotite or pyrite are local accessory phases. These meta-volcanic amphibolites form competent units during the high grade metamorphism: they are fractured and intruded by pegmatite veins/dykes, or, in the case of smaller occurrences, attenuated, boudinaged and/or dismembered.

LITHOLOGY - GRANITOIDS AND OTHER INTRUSIVES

Granitoid rocks are described in four main groups: Julianehåb batholith granites s.l., banded orthogneiss, autochthonous (S-type) granite, and rapakivi suite granites. The Julianehåb batholith, exposed in the northwest of the map sheet, is a *c.* 80 km wide zone consisting of a calc-alkaline suite of variably foliated granodiorite, granite and diorite containing a range of hornblende-bearing appinite dykes (Chadwick *et al.*, 1994). The tectonic setting of the batholith has recently been re-interpreted as a juvenile magmatic arc (Chadwick & Garde, in press). Banded orthogneiss occurs in the northeast of the map area, possibly as a sheet below or within the supracrustal sequence. The orthogneiss may represent an (early?) phase of the batholith suite. Autochthonous granites are largely in situ S-type rocks formed by partial melting within the meta-sedimentary sequence during the regional high T metamorphism. They occur on all scales, but larger bodies are more common towards the east coast. The late tectonic rapakivi suite consists of quartz-monzonite to syenite intrusions, with or without associated norite. The quartz-monzonites are regarded as lower crustal melts (Brown *et al.*, 1992).

Julianehåb batholith

Chadwick *et al.* (1994) described the various types of granodiorites and their textures, in the Julianehåb batholith on the west coast. Most of the batholith west and north-west of Danell Fjord is grey hornblende-biotite granodiorite similar to that in the Søndre Sermilik map sheet area. Appinite dykes are common: in net-veined complexes, or as foliated dykes with oblique fabrics indicating syntectonic emplacement. The batholith rocks are variably foliated and locally lineated, with a subvertical 060-trending fabric. Several plutons interpreted as part of the batholith suite have intruded the supracrustal sequence. A pluton south of the head of Danell Fjord shows development of a magmatic 'flow foliation', i.e. alignment of small feldspar phenocrysts within a matrix of unoriented minerals, parallel to the regional upright foliation within the batholith itself. North of central Lindenow Fjord a hornblende granodiorite with locally abundant appinite dykes can be traced north-east from the fjord for at least 20 kilometres. This granodiorite, locally with enclaves of mafic diorite, resembles those in the Julianehåb batholith. The appinite dykes are aligned parallel to the LS fabric defined by hornblende and stretched enclaves. In the north the well-developed linear fabric in the granodiorite is co-axial with the fold axes of upright, gently plunging and ENE-trending folds. In the south between the fjord and the 136 m lake, the granodiorite occupies the core of such a regional anticline.

Banded orthogneiss

Banded orthogneiss south of the mouth of Kangerluluk underlies amphibolite and psammite to the south with a largely concordant contact. They were derived by deformation of grey granodiorite (Julianahåb batholith?), and contain intercalations of abundant coarse feldspar as well as lenses of mafic diorite; some psammitic gneiss xenoliths may also be present. Grey granodiorite with scattered mafic lenses occurs between the supracrustal amphibolite and the orthogneiss immediately east of the Graah Fjelde rapakivi intrusion, but elsewhere sheared aplitic rocks (possible psammite?) are present along the contact itself. Whether this contact is tectonic, unconformable or intrusive is unclear. Chadwick (1992) mapped similar orthogneiss, with extensional shear zones dropping down to the south, to the north of the fjord.

Leucocratic granite

Autochthonous granite consists of leucocratic, feldspar porphyritic granite with many partially digested metasedimentary gneiss relics. They are S-type granites derived from the highly migmatitic gneiss during regional metamorphism. They occur in small bodies throughout the eastern part of the psammitic and pelitic gneisses, and form substantial sheets, for example along outer Kutseq.

Rapakivi suite

The late tectonic rapakivi suite granites include grey or more generally brown coloured quartz-monzonite (syenite) and less voluminous, dark norite, forming an essentially bimodal suite (Harrison *et al.*, 1990; Brown *et al.*, 1992). They are exposed in characteristic, spectacular mountains with sheer vertical walls more than 1 kilometre high, and occupy the high ground south-west and west of Danell and Lindenow Fjords. The Graah Fjelde - Kangerluluk Bjerge intrusion in the north east of the map sheet contains large, subhorizontal, metasedimentary gneiss xenoliths with pale hornfelsed rims and/or pale granite haloes. The pluton has consistent inward-dipping contacts, similar to the flat lower contacts of the mushroom-shaped pluton at the head of Lindenow Fjord described by Bridgwater *et al.* (1974). These contacts are strongly deformed, including, on the north side, the granite itself. Hutton *et al.* (1990) who worked further south in the Prins Christian Sund region, regarded the rapakivi plutons as sheets emplaced along regional extensional shear zones, with flats and ramps, traversing the supracrustal gneisses. Such regional shear zones have not been recognized within the Lindenow Fjord map sheet area. The Graah Fjelde - Kangerluluk Bjerge pluton is reported to have a U-Pb zircon age of *c.* 1755 Ma (Gulson & Krogh, 1975).

Mafic - ultramafic intrusive rocks

South of the head of Patussoq coarsely layered norite-monzonorite rocks form major outcrops. They contain amphibolite enclaves parallel to a magmatic foliation outlined by a preferred orientation of feldspar laths. Medium- to coarse-grained grey-green hornblende diorite, locally feldspar-phyric, occurs to the west, and is probably related to the norite. Norite-monzonorite and diorite both contain appinite dykes and shallow sheets of tourmaline-bearing granite. Both rock types are overlain by coarse syenite which borders the typically dark brown granites of the major rapakivi pluton west of Patussoq. The syenite is probably part of the rapakivi intrusion, whereas the norite-diorite rocks may be either rapakivi-related or associated with the Julianehåb batholith.

Only a few, larger mafic dykes are shown on the preliminary map. They include appinite dykes, which are generally interpreted as synplutonic with the Julianehåb batholith suite (Chadwick *et al.*, 1994) and occur throughout the supracrustal sequence in several generations. They consist of intermediate to mafic dykes characterized by hornblende phenocrysts. Several other, large mafic-ultramafic intrusions may also belong to the appinite group.

Some of the prominent unmetamorphosed Tertiary (?) dolerite-gabbro dykes with chilled margins and emplaced along east-and northeast-trending late stage faults and fractures are shown.

STRUCTURE

Folds in supracrustal sequence

An early phase of recumbent folding is inferred from flat-lying and/or refolded overturned sequences found in several localities. The largest area of overturning has been identified in the nunataks between Kutseq and Lindenow Fjord on the basis of primary structures in thin psammite beds intercalated with the vein quartz conglomerates. Smaller scale examples of overturning are found in semi-pelitic rocks, including the turbidite-like sequence west of Danell Fjord. Localised, small scale, often intrafolial, isoclines found elsewhere may be part of this early phase of folding. Although this early nappe-like folding is apparently widespread, its true scale is not yet fully assessed.

Open overturned folds with shallow north to north-west dipping axial planes are present on various scales in the Danell Fjord-Patussoq area and north of Lindenow Fjord. These folds include regional scale structures with kilometre-scale long limbs as well as outcrop scale structures. Axial planes are commonly accentuated by neosome veins (i.e. thin pegmatite dykes) or appinite veins, and the fold asymmetry suggests southwards directed movement. In the psammites south of Danell Fjord, axial planar pegmatite veins in these flat-lying folds overprint earlier pegmatite veins along the folded layering, and are themselves crosscut by ENE-trending subvertical pegmatite dykes. The relative timing of these folds remains to be resolved: do they predate, or are they contemporaneous with and transitional to, upright ENE-trending folds?

The ENE-trending, upright to steeply inclined folds with gentle north-east or south-west plunges dominate the map scale patterns. They are present as mesoscopic folds throughout the supracrustal sequence. In the turbiditic rocks west of Danell Fjord a subvertical upright foliation is well-developed as a crenulation cleavage in pelite and a spaced cleavage in psammite. In migmatitic psammites the folded migmatitic layering is often the dominant fabric, although pegmatite veins and dykes along the axial plane orientation can be commonly observed. In amphibolites the ENE-trending folds clearly deform an existing metamorphic fabric/layering, with or without a contained mineral lineation.

There are domains, e.g. in the area around eastern Kutseq, where the trend of these folds becomes more east-west (090) rather than east-northeast (060). Elsewhere, e.g. south of central Danell Fjord, upright folds locally trend more northerly (010-030). As stated earlier, the relationship between these upright folds and the earlier mentioned flat-lying folds is still being debated. Both styles of folding occurred at high metamorphic grade (axial planar pegmatite veins), fold an already recrystallized, high grade fabric, and appear at first glance to be mutually exclusive, although on a small scale there are possible overprinting criteria.

Late structures, developed mostly in pelitic rocks, include crenulation cleavages with both steep and shallow attitudes and local, broad open folds. They appear to postdate the metamorphic events because the microfolds and crenulation cleavage generally anastomoses around porphyroblasts. Weak crenulations south of inner Danell Fjord strike 140 with both, but mutually exclusive, northeasterly and southwesterly dips, both shallow and steep. Other directions include 090-striking open folds and microfolds associated locally with subvertical crenulations. For example, in the calc-silicate bearing psammite layers north of central Danell Fjord, flat-lying to very gently NNW-dipping isoclinal folds with subhorizontal fold axes are overprinted by upright, east-west striking folds with co-axial fold axes.

Contact relationships between Julianehåb batholith and supracrustal rocks

Several types of contacts between batholith plutons and supracrustal sequence have been observed, including intrusive, tectonic and possible unconformable contacts. Spectacularly exposed, virtually inaccessible flat-lying to gently dipping contacts in the Sorte Nunatak area are described by Chadwick (1992) and Chadwick & Garde (in press). On the north-east side, subhorizontal polymict conglomerate overlain by metabasalt and mafic greywacke may rest unconformably on granite of the Julianehåb batholith: a mafic dyke which cuts the granite, does not continue into the overlying supracrustal rocks. However, on the south-west side apophyses of the granite extend into the metabasalt-dominated sequence, although some shearing and quartz veining has occurred along the contact. The granite has a well-developed ENE-trending linear fabric. The north-western and south-eastern boundaries are subvertical, NE-trending shear zones, up to 100 m wide and include ultramylonites. Locally a large scale antiform with the same trend occurs adjacent to the north-western bounding fault of the Sorte Nunatak sequence.

Intrusive contacts between granodiorite of the Julianehåb batholith suite and semi-pelitic schist are found south-east of inner Danell Fjord. Here granodiorite contains a weak shape preferred orientation of feldspar parallel to the 060-trending structures which is interpreted as a magmatic foliation. The pluton has intruded after early deformation and high T metamorphism of the metasediments, and during the subsequent ENE-trending folding event. Another pluton of the batholith suite intruded into psammitic gneiss north of Lindenow Fjord. This granodiorite contains spectacular linear fabrics parallel to fold axes of the ENE-trending folds, and at least in the south lies in the core of an ENE-trending anticline. Banded granitoid gneiss at outer Kangerluluk may represent an earlier phase of the batholith, which may have intruded as a sheet into the supracrustal sequence, and possibly was affected by early subhorizontal deformation.

These various relationships may be explained by the long-lived nature of the batholith granite plutonism (50 - 100 Ma?; Chadwick & Garde, in press). Early, exposed phases of the batholith became both basement and source rock for the metasedimentary sequence. This sequence was intruded by early granodiorite sheets, and was then affected by high T - low P metamorphism and recumbent folding, before further plutons were emplaced during the ENE-trending upright folding.

The main batholith rocks have not recorded (and are probably not expected to record?) early subhorizontal planar deformation fabrics, but only show subvertical ENE-trending flow and solid state foliations, overprinted by shear zones and mylonites compatible with a sinistral transpressional regime.

Late stage faults

Late stage faults associated with brittle deformation textures (very fine brecciation, pseudo-tachylite?) and retrograde metamorphism (e.g. extensive epidote) postdate the main Ketilidian structures. Their real age is not known, and they could be related to Tertiary continental break-up (T.F.N. Nielsen, pers. comm.). The faults are responsible for many of the lineaments in the landscape, and probably controlled the present-day fjord system. Many are intruded by unmetamorphosed Tertiary (?) gabbro dykes. The main strike orientations are 100-110, 050-060 and 330. Left-lateral movement of 4-5 km can be inferred for a fault underlying Kangerluluk, based on the displacement of the northern and southern portions of the Graah Fjelde - Kangerluluk Bjerge rapakivi intrusion (see 1:500 000 South Greenland map sheet compiled by Allaart). Comparable sinistral displacement can be suggested for a fault underlying Danell Fjord, based on the apparent displacement of an amphibolite marker unit. East of Peer Vig in Lindenow Fjord, a 105-striking fault (Rolf fault) is intruded by a prominent gabbro dyke, and shows a sinistral displacement component of 400-500 meters measured by the off-set of an appinite dyke and amphibolite unit.

METAMORPHISM

The Ketilidian supracrustal sequence is characterized by low pressure regional metamorphism, and records high metamorphic grades as evidenced by the extensive partial melting in all meta-sedimentary lithologies. To the south of the map sheet, granulite facies conditions have been reached (e.g. Dawes, 1966; Wallis, 1966; Dempster *et al.*, 1991), but on the Lindenow Fjord map sheet area peak metamorphism occurred at upper amphibolite facies, with the exception of a narrow somewhat lower grade domain (lower or epidote amphibolite facies) along the Julianehåb batholith - supracrustal boundary.

The metamorphic grade of the supracrustal sequence increases away from the contact with the batholith. For example, turbiditic sequences west of the head of Danell Fjord have preserved the original sedimentary grain size variations in their graded beds: medium-grained psammite to fine-grained pelite. The deformed sequence contains many small quartz veins. Similar turbiditic rocks exposed in the core of a small anticline along the southern shore of central Danell Fjord are recrystallized at higher metamorphic grade: the pelite is converted into medium- to coarse-grained garnet-biotite-quartz-feldspar gneiss, whereas the psammite has largely retained its original medium grain size. These gneisses also contain numerous small quartzo-feldspathic neosome veins rather than quartz veins. In the migmatitic gneiss, the volume of neosome increases broadly towards the east and south-east.

The lower grade domain along the batholith boundary zone probably represents lower amphibolite (or epidote amphibolite) facies conditions. Metabasalt and mafic greywacke contain widespread epidote-hornblende assemblages. The semi-pelitic sequence west of Danell Fjord shows andalusite porphyroblasts which grow over, and are parallel to, a subvertical biotite-muscovite(?)-quartz-feldspar foliation, trending ENE.

To the east along the south coast of inner Danell Fjord, semi-pelitic schist and gneiss contain biotite-fibrolitic sillimanite assemblages defining the main fabric, and in addition contain scattered andalusite, K-feldspar and muscovite porphyroblasts. Preliminary microstructural observations indicate that these last three porphyroblasts (occurring in pairs: andalusite-muscovite and alkalifeldspar-muscovite) have grown across and enclosed trails of the sillimanite-biotite fabric. The porphyroblasts record a later, lower P-T metamorphic event than the early peak metamorphic biotite-sillimanite assemblage. Locally K-feldspar has grown over late stage crenulations, indicating the relatively late timing of this second thermal event.

At Peer Vig along the north coast of Lindenow Fjord, similar semi-pelitic gneiss contains fine-grained biotite-sillimanite with cordierite, garnet, and andalusite with muscovite porphyroblasts. Microstructures suggest - as one possible sequence of events - that early biotite-sillimanite is transitional to a biotite-sillimanite-cordierite-garnet assemblage representing a transition to granulite facies conditions. Late stage cordierite-quartz coronas on garnet, and andalusite and muscovite replacement of biotite-sillimanite, and lenses of medium-grained K-feldspar are again compatible with a second metamorphic event at lower P and T.

The preliminary microstructural evidence for an early high T event, accompanied by extensive partial melting, and followed by a distinctly lower P-T event needs further detailed study. There are suggestions of similar P-T histories in the reports from the west coast of South Greenland by Wallis (1966) and Dawes (1970), but apparently not from the granulite facies domain at Prins Christian Sund and Aappilattoq to the south of the Lindenow Fjord area (Dempster *et al.*, 1991). It is noteworthy that the peak metamorphic conditions in the lower grade domain apparently correlate (in grade and relative timing) with the second, lower grade event in the upper amphibolite facies domain. This second metamorphic event may record 'contact metamorphism' during emplacement of late stage batholith plutons into the supracrustal sequence.

CORRELATION WITH WEST COAST OF SOUTH GREENLAND

The supracrustal sequence in the Lindenow Fjord map sheet area represents the lateral continuation of the high grade metasedimentary and metavolcanic rocks in the Nanortalik -

Tasermiut areas along the west coast (Dawes, 1970; Escher, 1966; Wallis, 1966). The same lithologies are present, including the 'graphite-Fe sulphide-chemical sediment-amphibolite' association, calc-silicate facies in psammitic rocks, and the various rock types (flows, agglomerates, tuffaceous rocks, epiclastic rocks) in mafic volcanic units. On both the east and west coasts the thickest, best-preserved mafic sequences are found close to the Julianehåb batholith, and apparently at a high (structural-) stratigraphic level. None of the detailed studies on the west coast reported undoubted felsic volcanic rocks. Although these studies were made in very high grade domains, a comparison of migmatitic/pegmatitic textures, metamorphic developments and structural history is possible (with some translation of 1960s nomenclature into present day jargon).

In general, similar fold styles and trends are recognized in the same sequence of development on the west and east coasts. One interesting difference is the prominence of upright, open-close, NW-trending folds on the west coast, which predate and/or are contemporaneous with the ENE-trending folds (e.g. Wallis, 1966). On the east coast only rare NW-trending folds are developed in the western Lindenow Fjord area, and ENE-NE trending folds dominate.

Throughout the migmatitic supracrustal sequence, the earliest recognizable structures deform an already high grade fabric and/or have fine pegmatitic neosome along their axial plane. The high grade conditions were maintained during subsequent folding stages. The exception to this rule is found in the relatively low grade rocks (i.e. low amphibolite facies) directly along the batholith contact, where andalusite porphyroblasts appear to have overgrown the subvertical ENE-trending foliation. The very early timing of the high grade metamorphism, as well as its regional distribution (i.e. not related to either Julianehåb batholith or the rapakivi suite) have implications for the tectonic setting: (very) high heat flow soon after deposition and/or during early deformation needs to be explained.

ECONOMIC GEOLOGY

Reconnaissance geochemical mapping

Geochemical mapping based on stream sediments along the west coast of South Greenland led to the recognition of geochemical provinces that correlate well with regional lithotectonic zones (Armour-Brown *et al.*, 1982, 1984; Steenfelt & Armour-Brown, 1988; Steenfelt & Tukiainen, 1991). The same geochemical provinces, based on a relatively small number of stream sediment samples collected during SUPRASYD 1992, can be recognized along the east coast of South Greenland, and follow the major lithotectonic subdivision of the Ketilidian orogen (Steenfelt *et al.*, 1992). In general, a geochemical break between two 'provinces' lies just south of the mapped contact between the Julianehåb batholith and the migmatitic supracrustal rocks.

	high concentrations	low concentrations
Julianehåb batholith	Al,V,Ti,P,Sr,Na,Ba	Cr,Sb,Ni
Supracrustal rocks	As,Au,Cs,Rb,Sb,Sm,Th,U,W,Y,Yb	Sr,P,Ba

The geochemical mapping studies concluded that both the Julianehåb batholith and migmatitic supracrustal sequence are part of Ketilidian gold and uranium geochemical provinces (Armour-Brown *et al.*, 1982, 1984; Steenfelt & Armour-Brown, 1988; Steenfelt & Tukiainen, 1991; Steenfelt *et al.*, 1992; Thorning *et al.*, 1994). In general the supracrustal sequence is characterized by elevated background levels of U as well as Au, As, and Sb (Steenfelt & Tukiainen, 1991).

Selected rock and stream sediment anomalies are shown on the preliminary geological map (enclosed Map 1). These data have been compiled from Armour-Brown *et al.* (1982), Ferguson & Rowntree (1994), Steenfelt *et al.* (1992) and from results of the SUPRASYD 1992 and 1994 field seasons. Geochemical results from the 1994 samples are shown in the Tables 1-3.

Mineralization systems

Several types of mineralization systems are distinguished: (1) a stratabound 'graphite - Fe-sulphide - chemical sediment - amphibolite' association within psammite, which can be subdivided into a 'pelitic graphitic shale' association and a 'metalliferous black shale' association, (2) a similar stratabound mineralization with graphitic-sulphidic intervals, contained entirely within mafic and ultramafic metavolcanic rocks, (3) crosscutting veins in mafic metavolcanic rocks, (4) shear zones in the boundary zone of the Julianehåb batholith and the supracrustal rocks, and (5) uranium mineralization in migmatitic psammitic gneiss, particularly in the southern part of the Lindenow Fjord map sheet.

1) The 'graphite - Fe sulphide - chemical sediment - amphibolite' association represents a distinct depositional environment characterized by highly reduced or no supply of clastic felsic material, and by chemical sedimentation with minor or substantial mafic volcanic/volcaniclastic rocks. These deeply rusty weathered layers stand out amongst the lighter coloured psammitic and semi-pelitic gneisses. Pyrrhotite or pyrite are the dominant sulphides, with minor chalcopyrite and sphalerite. The graphitic - slaty beds are commonly strongly deformed, and may be extensively quartz veined. This association could act as a preferential host for epigenetic Au mineralization.

Graphitic schist layers and lenses of the general 'pelitic graphitic shale' association are present throughout the clastic supracrustal sequence (e.g. north of central Daneel Fjord, Fig. 2A). Geochemically they are characterized by variably raised background levels for Au (max. 33 ppb) and locally elevated levels for As (max. 130 ppm) and Zn (max. 1585 ppm), but contain low levels of the other elements that are high in the Stendalen occurrence discussed below.

The metalliferous 'black shale' association is represented by a prominent gossanous layer east of Stendalen, on the north shore of inner Lindenow Fjord. Geochemical analyses show typically relatively high values for a range of elements including Au, As, Cu, Zn, Ni, Mo, Se, U and V (cf. sample numbers 412915-916, 413019-021 in Table 2). In contrast the contents in Pb and Ba are low, suggesting reduced input of terrigenous material. The Stendalen graphitic schist occurrence lies directly above a contact with intrusive granite which contains 'enclaves' of mafic-ultramafic rocks. These may originally have underlain the Stendalen graphitic schist.

2) Stratabound alteration, indicated by rusty weathering horizons, is associated with pyroclastic beds and chemical (interflow) sediment layers within mafic (e.g. south of Kutseq; west of Kangerluk) and ultramafic (Illukulik) metavolcanic sequences. South of Kutseq carbonate altered pillow structures are well preserved within a regionally persistent amphibolite layer that is characterized by elevated levels of As (Fig. 2B). A chip sample over 3 m across one of these layers contains 12 ppb Au and 184 ppm As. A chip sample of an adjacent, 30 cm thick, pyroclastic layer, now consisting of biotite-hornblende-quartz-feldspar schist with visible arsenopyrite and pyrrhotite, contains 1.1% As and 77 ppb Au, whereas a grab sample from the same horizon yielded 1.7% As and 179 ppb Au.

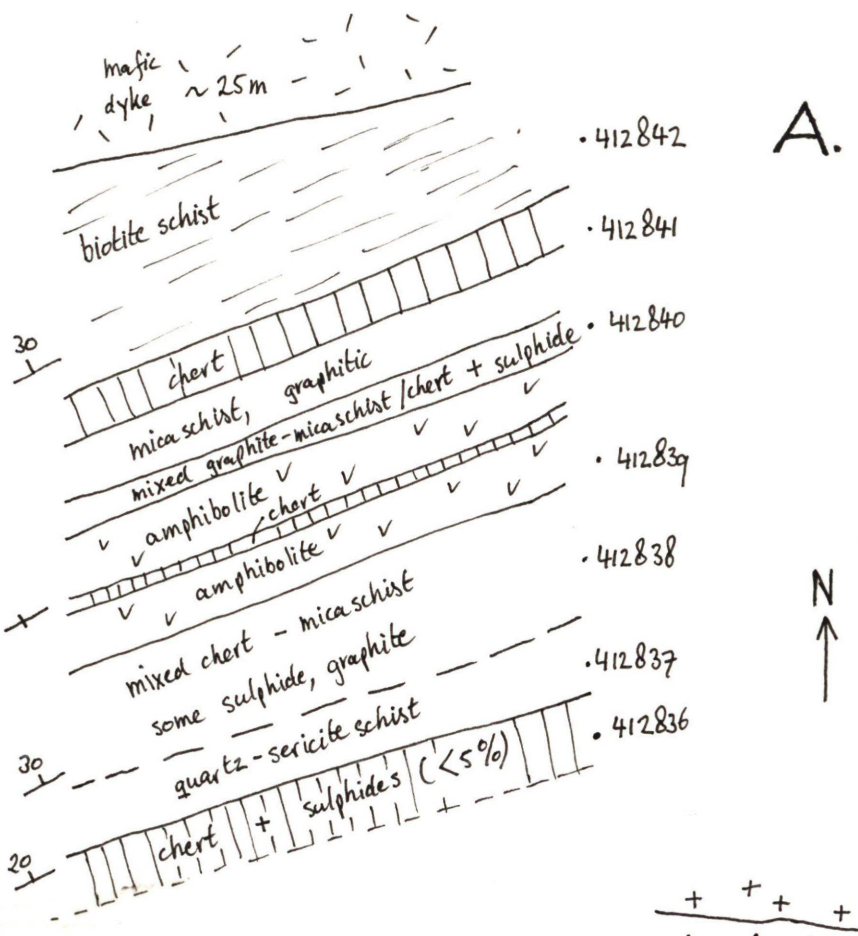

Figure 2A. Sketch map of rusty pelitic - mafic volcanic sequence, north of central Danell Fjord. With location of sample numbers.

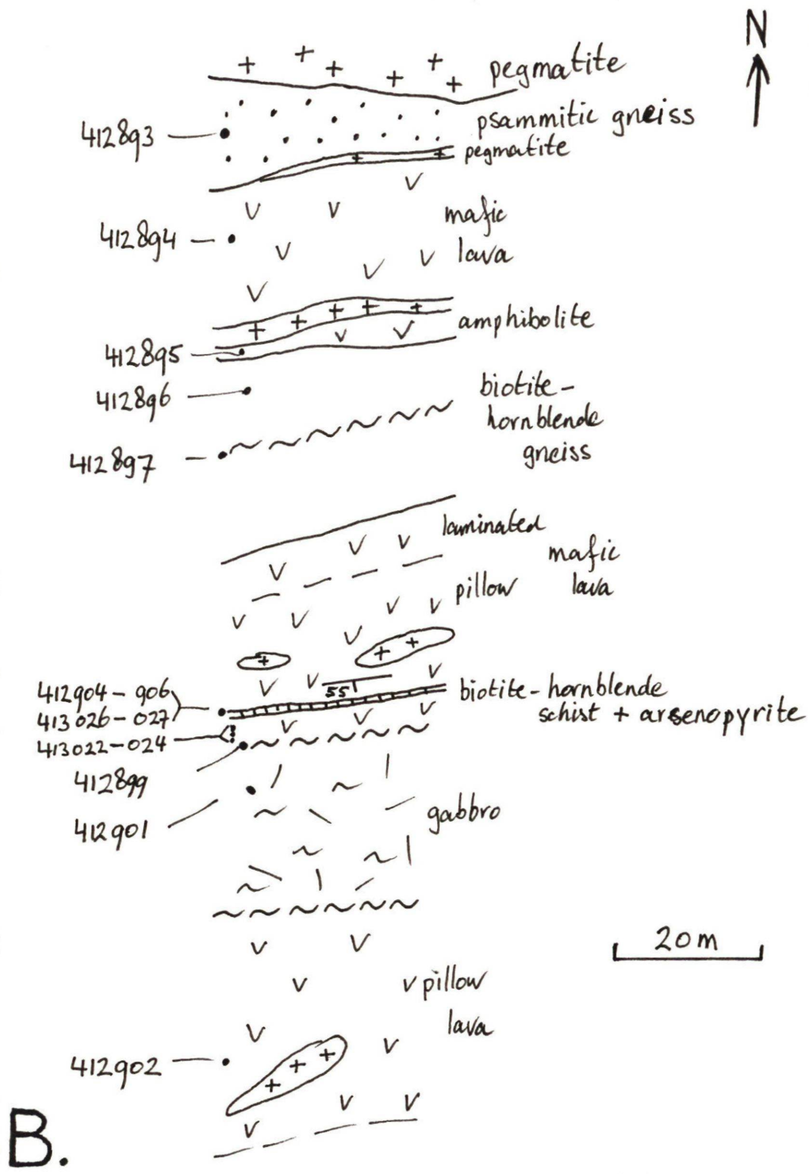

Figure 2B. Sketch map of amphibolitic mafic volcanic sequence south of Kutseq, showing location of sample numbers.

An amphibolite unit east of Illukulik on the north shore of Lindenow Fjord consists ofinterleaved massive layers and graphitic mafic schist, possibly derived from volcaniclastic rocks and containing possible chemical sediment layers. All rocks in this sequence have ultramafic, rather than mafic, geochemical signatures: high Ni (max. 0.1%), Cr (max. 0.16%), MgO (*c.* 20%), SiO2 (43-47%) and Mg/Fe ratio (1.25-1.45). In addition, elevated values are found for Au (max. 40 ppb), As (max. 200 ppm) and Sb (max. 110 ppm). Typically Ba and Pb have low values.

The same ultramafic association has been found in supracrustal inliers in rapakivi granite at Illorsuit (sample number 412880). Furthermore, similar ultramafic rocks are present underlying the Stendalen metalliferous graphitic-sulphidic schist which itself is characterized by very low Pb and Ba (sample numbers 412912-914). Possibly the three occurrences represent the same stratigraphic layer of which the original section included a lower ultramafic volcanic/volcaniclastic part overlain by a metalliferous black shale.
It should be noted that this stratabound mineralization can be regarded as the mafic volcanic dominated end-members of the 'graphite - Fe sulphide - chemical sediment - amphibolite' association.

3) Mafic volcanic rocks locally contain high Au and Cu values (up to 9 ppm and 4% respectively) in narrow quartz and/or carbonate veins in little deformed meta-basalt boulders from Sorte Nunatak to the northwest of the head of Danell Fjord (Appel, 1992; Ferguson & Rowntree, 1994). Appel (1992) recorded minor carbonate alteration with numerous 'hairline' cracks which also show malachite staining. However, more substantially mineralized, sheeted or simple, quartz veins along shear zones in competent amphibolitized metabasaltic units (i.e. as the Nalunaq prospect on the west coast: Gowen *et al.*, 1993) have not been found.

4) Regional retrograde shearzones along the southeast margin of the Julianehåb batholith have been recognized as possible sites for substantial gold mineralization (Garde & Schønwandt, 1994; Schønwandt, 1994; Stendal *et al.*, in press). Stendal *et al.* (in press) documented Au-Bi-W-Cu-(Mo-Sn) element associations - in various combinations - within the Niaqornaarsuk shear zone system. The shear zone occurs in the southern part of the batholith where granite is interleaved with various supracrustal lithologies, including felsic subvolcanic rocks. Most of the mineralization occurs in second order shear zones with quartz veins in amphibolite and in granitoids.

Only limited reconnaissance of such zones has so far been carried out on the Lindenow Fjord map sheet area. A major shear zone northwest of inner Danell Fjord lies along the boundary between the batholith and the supracrustal sequence. The shear zone is developed in diorite, and is characterized by carbonate alteration and quartz veining. A minor raise in Au values has been documented (max. 217 ppb Au), but only one incomplete section has been sampled across this major shear zone. However, a narrow (2 cm wide) shear zone in granite north of western Kangerluluk with a chalcopyrite- and pyrite-bearing quartz vein contains relatively high Cu-Au (0.4% - 0.6 ppm), and indicates the potential for this type of mineralization.

5) Uranium mineralization appears to be mainly associated with the migmatitic supracrustal sequence. Just south of the map sheet area the Illorsuit uranium prospect (Armour-Brown, 1986) contains disseminated and fracture-controlled, stratabound high grade uraninite mineralization within meta-psammite/arkose (with conglomerate, graphitic-sulphidic schist) and intermediate meta-volcanic (amphibolite) rafts within rapakivi granite. Armour-Brown (1986) argued that uranium was present in the supracrustal units before deformation, metamorphism and rapakivi intrusion, and has been remobilized into structurally controlled sites (e.g. fold hinges) during regional deformation and migmatization.

REFERENCES

Allaart, J. H. 1975: Geological map of Greenland 1:500 000, sheet 1, Sydgrønland. Copenhagen: Geological Survey of Greenland.

Allaart, J. H. 1976: Ketilidian mobile belt in South Greenland. *In* Escher, A. & Watt, W. S. (ed.) *Geology of Greenland.* Copenhagen: 603 pp. Grønlands geol. Unders.

Andrews, J. R., Bridgwater, D., Gormsen, K., Gulson, B. L., Keto, L. & Watterson, J. 1973: The Precambrian of South-East Greenland. *In* R. G. Park & J. Tarney (Ed.) *The Lewisian of Scotland and related rocks of Greenland*, University Press Birmingham, 143-156.

Appel, P. W. U. 1992: Field diary 1992. Unpublished report, Grønlands geol. Unders., 21 pp.

Appel, P. W. U. & Lind, M. 1993: Gold Exploration on the Nanortalik Peninsula, South Greenland. *Open File Ser. Grønlands geol. Unders.* **93/3**, 66 pp.

Armour-Brown, A. 1986: Geology and evaluation of the uranium mineralization at Igdlorssuit, South Greenland. Unpublished report, Grønlands geol. Unders., 60 pp.

Armour-Brown, A., Tukiainen, T. & Wallin, B. 1982: The South Greenland uranium exploration program. Final Report. Unpublished report, Grønlands geol. Unders., 95 pp.

Armour-Brown, A., Tukiainen, T., Nyegaard, P. & Wallin, B. 1984: The South Greenland exploration programme. Final Report of progress 1980-1983. Unpublished report, Grønlands geol. Unders., 107 pp.

Bridgwater, D., Sutton, J. & Watterson, J. 1974: Crustal downfolding associated with igneous activity. *Tectonophysics* **21**, 57-77.

Brown, P. E., Dempster, T. J., Harrison, T. N. & Hutton, D. H. W. 1992: The rapakivi granites of South Greenland - crustal melting in response to extensional tectonics and magmatic underplating. *Trans. Royal Soc. Edinburgh Earth Sciences* **83**, 173-178.

Chadwick, B. 1992: Field report Suprasyd 1992. Unpublished report, Geological Survey of Greenland, 23 pp.

Chadwick, B. 1994: Field report Suprasyd 1994: Report on fieldwork in the Ketilidian orogen during the summer of 1994. Unpublished report, Geological Survey of Greenland, 16 pp.

Chadwick, B. & Garde, A. A. in press: Palaeoproterozoic oblique collision in South Greenland: A reappraisal of the Ketilidian Orogen. *In* T. S. Brewer & B. P. Atkin (Ed.) *Precambrian crustal evolution in the North Atlantic Regions*, Spec. Publ. Geol. Soc. London.

Chadwick, B., Erfurt, P., Frisch, T., Frith, R. A., Garde, A. A., Schønwandt, H. K., Stendal, H. & Thomassen, B. 1994: Sinistral Transpression and Hydrothermal Activity During Emplacement of the Early Proterozoic Julianehåb Batholith: Ketilidian Belt, South Greenland. *Rapp. Grønlands geol. Unders.* **163**, 5-22.

Chadwick, B., Erfurt, P., Frith, R. A., Nielsen, T. F. D., Schønwandt, H. K. & Stendal, H. 1994: Reappraisal of the Ikermit supracrustal suite of the Ketilidian border zone in South-east Greenland. *Rapp. Grønlands geol. Unders.* **163**, 23-31.

Dawes, P. R. 1966: *The genesis of rapakivi granite and its position in the evolution of the Precambrian of the Tasiussak area, South Greenland.* Unpublished Ph.D. thesis, University of Exeter.

Dawes, P. R. 1966: The plutonic history of the Tasiussaq area, South Greenland. *Bull. Grønlands geol. Unders.* **59**, 125 pp.

Dempster, T. J., Harrison, T. N., Brown, P. E. & Hutton, D. H. W. 1991: Low Pressure granulites from the Ketilidian Mobile belt of Southern Greenland. *Jl. Petrology* **32**, 979-1004.

Dempster, T. J., Hutton, D. H. W., Harrison, T. N., Brown, P. E. & Jenkin, G. R. T. 1991b: Textural evolution of rapakivi granites, south Greenland. *Contr. Min. Petr.* **107**, 459-471.

Erfurt, P. 1992: Feltrapport og dagbog - Suprasyd 1992. Unpublished report, Geological Survey of Greenland, 9 pp.

Escher, A. 1966: The deformation and granitisation of Ketilidian rocks in the Nanortalik area, South Greenland. *Bull. Grønlands geol. Unders.* **59**, 102 pp.

Ferguson, J. & Rowntree, J. C. 1994: Report on Exploration Licence 11/93 Lindenow Fjord and Prospecting Licence 09/93. Unpubl. intern. rep. Quadrant Resources Pty. Ltd. 7 pp.

Frith, R. A. 1992: Field report Suprasyd 1992. Unpublished report, Geological Survey of Greenland, 34 pp.

Garde, A. A. & Schønwandt, H. K. 1994: Project SUPRASYD 1993 - granitic rocks and shear zones with possible gold potential, Julianehåb batholith, South Greenland. *Rapp. Grønlands geol. Unders.* **160**, 28-31.

Garde, A. A. & Schønwandt, H. K. in press: Project SUPRASYD 1994 - Ketilidian supracrustal rocks in South-East Greenland and gold-bearing shear zones in the Julianehåb batholith. *Rapp. Grønlands geol. Unders.*

Gowen, J., Christiansen, O., Grahl-Madsen, L. & Pedersen, J. 1993: Discovery of the Nalunaq Gold Deposit, Kirkespirdalen, S.W. Greenland. *International Geology Review* **35**, 1001-1008.

Gulson, B. L. & Krogh, T. E. 1975: Evidence of multiple intrusion, possible resetting of U-Pb ages, and new crystallization of zircons in the post-tectonic intrusions ('Rapakivi granites') and gneisses from South Greenland. *Geochim. Cosmochim. Acta* **39**, 65-82.

Harrison, T. N., Reavy, R. J., Finch, A. A. & Brown, P. E. 1990: Co-existing mafic and felsic magmas in the early Proterozoic rapakivi granite suite of Southern Greenland. *Bull. Geol. Soc. Denmark* **38**, 53-58.

Hutton, D. H. W., Dempster, T. J., Brown, P. E. & Becker, S. D. 1990: A new mechanism of granite emplacement: Greenland rapakivi intrusions in active extensional shear zones. *Nature* **343**, 452-455.

Kalsbeek, F. 1994: Archaean and Proterozoic basement provinces in Greenland. *Rapp. Grønlands geol. Unders.* **160**, 37-40.

Kalsbeek, F. & Taylor, P. N. 1985: Isotopic and chemical variation in granites across a Proterozoic continental margin - the Ketilidian mobile belt of South Greenland. *Earth Planet. Science Lett.* **73**, 65-80.

Kalsbeek, F., Larsen, L. M. & Bondam, J. 1990: Sydgrønland Sheet 1, Geology map of Greenland 1:500 000 Descriptive text, Grønlands geol. Unders., 36 pp.

Nielsen, T., Chadwick, B., Dawes, P., Frith, R. & Schønwandt, H. K. 1993: Project SUPRASYD 1992: opening season in the Ketilidian of South Greenland. *Rapp. Grønlands geol. Unders.* **159**, 25-31.

Patchett, P. J. & Bridgwater, D. 1984: Origin of the continental crust of 1.9-1.7 Ga age defined by Nd isotopes in the Ketilidian terrain of South Greenland. *Contr. Miner. Petrol.* **87**, 311-318.

Pedersen, S., Larsen, O., Bridgwater, D. & Watterson, J. 1974: Rb/Sr whole rock isochron age determinations on metamorphosed acid volcanic rocks and granitic gneisses from the Ketilidian mobile belt, South-east Greenland. *Rapp. Grønlands geol. Unders.* **66**, 12-22.

Schønwandt, H. K. 1994: Mineral Resource activities 1993: spectrum of research and services. *Rapp. Grønlands geol. Unders.* **160**, 18-21.

Steenfelt, A. & Tukiainen, T. 1990: Geochemical Mapping: distribution of gold, arsenic, antimony and tantalum in South Greenland. *Rapp. Grønlands geol. Unders.* **152**, 55-61.

Steenfelt, A. 1990: Gold content of regional stream sediment samples from South Greenland. *Open File Ser. Grønlands geol. Unders.* **90/5**, 12 pp.

Steenfelt, A., Dam, E. & Erfurt, P. 1992: Reconnaissance geochemical mapping of eastern South Greenland (60°30′ to 62°30′N). *Open File Ser. Grønlands geol. Unders.* **92/10**, 15 pp.

Stendal, H., Grahl-Madsen, L., Olsen, H. K., Schønwandt, H. K. & Thomassen, B. in press: Gold exploration in the early Proterozoic Ketilidian orogen, South Greenland. *Journal Geol. Soc. CIM - Explor. and Min. Geol.*

Swager, C. 1995: Field report Suprasyd 1994: Ketilidian high grade metasedimentary sequences along the Danell and Lindenow Fjords, Southern Greenland, and some observations from the Søndre Sermilik area. Unpublished report, Geological Survey of Greenland, 27 pp.

Thorning, L., Tukiainen, T. & Steenfelt, A. (ed.) 1994: Regional compilations of geoscience data from the Kap Farvel - Ivittuut area, South Greenland. *Thematic Map Series No.* **94/1** (Parts A and B) Grønlands geol. Unders.

Tukiainen, T., Erfurt, P. & Thorning, L. 1993: Project to assess the application of Spot and Landsat TM imageries to geological reconnaissance, South-East Greenland - Final Report. *Open File Ser. Grønlands geol. Unders.* **93/8**, 32 pp.

Van Breemen, O., Aftalion, M. & Allaart, J. H. 1974: Isotopic and geochronologic studies on granites from the Ketilidian mobile belt of South Greenland. *Bull. Geol. Soc. Am.* **85**, 403-412.

Wallis, R. H. 1966: *Geology of North-east Tasermiut Fjord, South Greenland.* Unpublished Ph.D. thesis, University of Birmingham.

Windley, B. F. 1991: Early Proterozoic Collision Tectonics and Rapakivi Granites as Intrusions in an Extensional Thrust-Thickened Crust: The Ketilidian Orogen, South Greenland. *Tectonophysics* **195**, 1-10.

Table 1. Analytical methods and detection limits.

All analyses are by Activation Laboratories Ltd., Ontario. The following methods have been used:

(1) Instrumental neutron activation analyses

Rock samples, stream sediment samples

Element	Detection limit		Element	Detection limit	
Au	2	PPB	Na	0.01	PCT
Ag	5	PPM	Ni	20	PPM
As	0.5	PPM	Nd	5	PPM
Ba	50	PPM	Rb	5	PPM
Br	0.5	PPM	Sb	0.1	PPM
Ca	1	PCT	Sc	0.1	PPM
Ce	3	PPM	Se	3	PPM
Co	1	PPM	Sm	0.1	PPM
Cr	5	PPM	Sn	0.01	PPM
Cs	1	PPM	Sr	500	PPM
Eu	0.2	PPM	Ta	0.5	PPM
Fe	0.01	PCT	Th	0.2	PPM
Hf	1	PPM	Tb	0.5	PPM
Hg	1	PPM	U	0.5	PPM
Ir	5	PPB	W	1	PPM
La	0.5	PPM	Zn	50	PPM
Lu	0.05	PPM	Yb	0.2	PPM

(2) Aqua regia extraction/inductively coupled plasma emission spectrometry (icp)

Rock samples, stream sediment samples

Element	Detection limit				
Ag	0.5	PPM	Mo	2	PPM
Al	0.01	PCT	Ni	1	PPM
Be	2	PPM	P	0.001	PCT
Bi	5	PPM	Pb	5	PPM
Ca	0.01	PCT	Sr	1	PPM
Cd	0.5	PPM	Ti	0.01	PCT
Cu	1	PPM	V	2	PPM
K	0.01	PCT	Y	2	PPM
Mg	0.01	PCT	Zn	1	PPM
Mn	1	PPM			

Note. 0 or 0.0 in the analytical results indicates a value below the detection limit.

Table 1. Analytical methods and detection limits.

(3) Instrumental neutron activation analyses

Heavy mineral concentrates

Element	Detection limit		Element	Detection limit	
Au	5	PPB	Mo	20	PPM
Ag	5	PPM	Na	0.05	PCT
As	2	PPM	Nd	10	PPM
Ba	200	PPM	Ni	200	PPM
Br	5	PPM	Rb	50	PPM
Ca	1	PCT	Sb	0.2	PPM
Ce	3	PPM	Sc	0.1	PCT
Co	5	PPM	Se	20	PPM
Cr	10	PPM	Sm	0.1	PPM
Cs	2	PPM	Sr	0.2	PCT
Eu	0.2	PPM	Ta	1	PPM
Fe	0.02	PCT	Tb	2	PPM
Hf	1	PPM	Th	0.5	PPM
Hg	5	PPM	U	0.5	PPM
Ir	50	PPB	W	4	PPM
La	1	PPM	Yb	0.2	PPM
Lu	0.05	PPM	Zn	200	PPM

(4) Aqua regia extraction/inductively coupled plasma emission spectrometry (icp)

Heavy mineral concentrates

Element	Detection limit	
Ag	0.2	PPM
Cd	0.5	PPM
Cu	1	PPM
Mn	2	PPM
Ni	1	PPM
Pb	2	PPM
Zn	1	PPM

(5) Lead fire assay/icp analysis (fa)

Rock samples

Element	Detection limit	
Au	1	PPB
Pd	3	PPB
Pt	5	PPB

Table 2. Rock samples

GGU no	Locality	Altitude metre	Type
411614	Danell Fjord		Hand sample
411615	Danell Fjord		Hand sample
411617	Danell Fjord		Hand sample
411639	Danell Fjord		Hand sample
411645	Danell Fjord		Hand sample
411654	Danell Fjord		Hand sample
412007	Kangerluluk	600	Hand sample
412807	Danell Fjord	150	Hand sample
412808	Danell Fjord	190	Chip sample: 1.0 m
412809	Danell Fjord	1100	Chip sample: 0.5 m
412810	Danell Fjord	1100	Hand sample
412811	Danell Fjord	1100	Hand sample
412812	Danell Fjord	1100	Hand sample
412813	Danell Fjord	1100	Hand sample
412814	Danell Fjord	1080	Hand sample
412815	Danell Fjord	1080	Hand sample
412816	Danell Fjord	1080	Chip sample
412817	Danell Fjord	1070	Chip sample: 1.5 m
412818	Danell Fjord	1070	Hand sample
412819	Danell Fjord	1060	Hand sample
412820	Danell Fjord	1060	Hand sample
412821	Danell Fjord	1060	Hand sample
412822	Danell Fjord	1060	Chip sample
412823	Danell Fjord	1060	Chip sample: 1.0 m
412824	Danell Fjord	1060	Chip sample
412825	Danell Fjord	1050	Chip sample: 2.0 m
412826	Danell Fjord	1050	Hand sample
412827	Danell Fjord	5	Chip sample: 0.5 m
412828	Danell Fjord	5	Hand sample
412829	Danell Fjord	30	Hand sample
412830	Danell Fjord	30	Hand sample
412831	Danell Fjord	70	Hand sample
412832	Danell Fjord	5	Hand sample
412833	Danell Fjord	5	Hand sample
412834	Danell Fjord	5	Hand sample
412835	Danell Fjord	5	Hand sample
412836	Danell Fjord	610	Hand sample
412837	Danell Fjord	610	Hand sample
412838	Danell Fjord	610	Hand sample
412839	Danell Fjord	610	Hand sample
412840	Danell Fjord	610	Hand sample
412841	Danell Fjord	610	Hand sample
412842	Danell Fjord	620	Hand sample
412843	Danell Fjord	680	Hand sample
412844	Danell Fjord	30	Chip sample: 1.5 m
412845	Danell Fjord	5	Hand sample
412846	Danell Fjord	5	Hand sample

Table 2. Rock samples

GGU no	Locality	Altitude metre	Type
412847	Danell Fjord	5	Chip sample: 3.0 m
412848	Danell Fjord	5	Hand sample
412849	Danell Fjord	5	Chip sample: 1.0 m
412850	Danell Fjord	5	Chip sample: 1.0 m
412851	Danell Fjord	5	Hand sample
412852	Kangerluluk	370	Hand sample
412853	Kangerluk	350	Hand sample
412854	Kangerluk	350	Chip sample: 5.0 m
412855	Kangerluk	360	Chip sample: 0.3 m
412856	Kangerluk	360	Hand sample
412857	Kangerluk	370	Chip sample: 0.5 m
412858	Kangerluk	370	Hand sample
412859	Kangerluk	380	Hand sample
412860	Kangerluk	670	Chip sample: 2.0 m
412861	Kangerluk	670	Hand sample
412862	Kangerluk	660	Hand sample
412863	Kangerluk	620	Hand sample
412864	Kangerluk	610	Hand sample
412865	Danell Fjord	100	Hand sample
412866	Danell Fjord	20	Hand sample
412867	Danell Fjord	20	Chip sample: 0.4 m
412868	Nørrearm	5	Hand sample
412869	Nørrearm	20	Chip sample
412870	Nørrearm	20	Chip sample: 6.0 m
412871	Nørrearm	5	Chip sample: 1.0 m
412872	Nørrearm	5	Chip sample: 1.2 m
412873	Nørrearm	5	Chip sample: 0.9 m
412874	Nørrearm	20	Chip sample: 1.0 m
412875	Nørrearm	5	Hand sample
412876	Nørrearm	20	Hand sample
412877	Illorsuit	650	Hand sample
412878	Illorsuit	550	Hand sample
412879	Illorsuit	500	Hand sample
412880	Illorsuit	500	Hand sample
412881	Peer Vig	70	Hand sample
412882	Lindenow Fjord	15	Hand sample
412883	Lindenow Fjord	15	Hand sample
412884	Lindenow Fjord	10	Hand sample
412885	Kangerluluk	470	Hand sample
412886	Lindenow Fjord	160	Hand sample
412887	Lindenow Fjord	250	Hand sample
412888	Lindenow Fjord	250	Hand sample
412889	Stendalen	25	Hand sample
412890	Lindenow Fjord	50	Chip sample: 1.0 m
412891	Lindenow Fjord	30	Hand sample
412892	Lindenow Fjord	10	Hand sample
412893	Kutseq Fjord	540	Hand sample

Table 2. Rock samples

GGU no	Locality	Altitude metre	Type
412894	Kutseq Fjord	540	Hand sample
412895	Kutseq Fjord	550	Chip sample
412896	Kutseq Fjord	550	Hand sample
412897	Kutseq Fjord	550	Chip sample: 2.0 m
412898	Kutseq Fjord	550	Hand sample
412899	Kutseq Fjord	550	Hand sample
412901	Kutseq Fjord	550	Hand sample
412902	Kutseq Fjord	550	Hand sample
412903	Kutseq Fjord	560	Chip sample: 3.0 m
412904	Kutseq Fjord	560	Chip sample: 0.4 m
412905	Kutseq Fjord	560	Hand sample
412906	Kutseq Fjord	560	Chip sample: 0.2 m
412907	Illukulik	90	Hand sample
412908	Illukulik	90	Hand sample
412909	Illukulik	90	Hand sample
412910	Illukulik	90	Chip sample
412911	Kangerluluk	1000	Hand sample
412912	Stendalen	50	Hand sample
412913	Stendalen	160	Hand sample
412914	Stendalen	190	Hand sample
412915	Stendalen	230	Hand sample
412916	Stendalen	230	Hand sample
413001	Danell Fjord	20	Hand sample
413002	Danell Fjord	2	Hand sample
413003	Danell Fjord	30	Hand sample
413004	Danell Fjord	40	Hand sample
413005	Danell Fjord	40	Hand sample
413006	Danell Fjord	40	Hand sample
413007	Danell Fjord	40	Hand sample
413008	Danell Fjord	630	Hand sample
413009	Danell Fjord	630	Hand sample
413010	Danell Fjord	680	Hand sample
413011	Danell Fjord	690	Hand sample
413012	Sønderarm	580	Hand sample
413013	Peer Vig	10	Hand sample
413014	Sorte Nunatak	300	Hand sample
413015	Kangerluluk	450	Hand sample
413016	Lindenow Fjord	160	Hand sample
413017	Lindenow Fjord	150	Hand sample
413018	Lindenow Fjord	170	Hand sample
413019	Lindenow Fjord	170	Hand sample
413020	Lindenow Fjord	170	Hand sample
413021	Lindenow Fjord	170	Hand sample
413022	Kutseq Fjord	560	Chip sample: 1.5 m
413023	Kutseq Fjord	560	Chip sample: 0.5 m
413024	Kutseq Fjord	560	Chip sample: 3.0 m
413025	Kutseq Fjord	540	Hand sample

Table 2. Rock samples

GGU no	Locality	Altitude metre	Type
413026	Kutseq Fjord	550	Hand sample
413027	Kutseq Fjord	560	Chip sample: 0.3 m
413028	Kutseq Fjord	940	Hand sample
413029	Kutseq Fjord	940	Hand sample

Table 2. Rock samples

GGU no	Design	Other information	Weight
411614			
411615			
411617			
411639		Ore mineral	
411645		Ore mineral	
411654			
412007			2 - 5 kg
412807		Ore mineral	0 - 2 kg
412808		Ore mineral	0 - 2 kg
412809	Stratigraphy	Representative	0 - 2 kg
412810	Stratigraphy	Representative	0 - 2 kg
412811	Stratigraphy	Representative	0 - 2 kg
412812	Stratigraphy	Representative	0 - 2 kg
412813	Stratigraphy	Representative	0 - 2 kg
412814	Stratigraphy	Representative	0 - 2 kg
412815	Stratigraphy	Representative	0 - 2 kg
412816	Stratigraphy	Representative	0 - 2 kg
412817	Stratigraphy	Representative	0 - 2 kg
412818	Stratigraphy	Representative	0 - 2 kg
412819	Stratigraphy	Representative	0 - 2 kg
412820	Stratigraphy	Representative	0 - 2 kg
412821	Stratigraphy	Representative	
412822	Stratigraphy	Representative	0 - 2 kg
412823	Stratigraphy	Representative	0 - 2 kg
412824	Stratigraphy	Representative	0 - 2 kg
412825	Stratigraphy	Representative	0 - 2 kg
412826	Stratigraphy	Ore mineral	0 - 2 kg
412827	Stratigraphy	Representative	0 - 2 kg
412828		Representative	
412829		Representative	0 - 2 kg
412830		Representative	0 - 2 kg
412831		Representative	0 - 2 kg
412832		Loose block	0 - 2 kg
412833		Representative	0 - 2 kg
412834		Loose block	0 - 2 kg
412835		Representative	0 - 2 kg
412836	Stratigraphy	Representative	0 - 2 kg
412837	Stratigraphy	Representative	0 - 2 kg
412838	Stratigraphy	Representative	0 - 2 kg
412839	Stratigraphy	Representative	0 - 2 kg
412840	Stratigraphy	Representative	0 - 2 kg
412841	Stratigraphy	Representative	0 - 2 kg
412842	Stratigraphy	Representative	0 - 2 kg
412843	Stratigraphy	Representative,weathered	0 - 2 kg
412844		Representative	0 - 2 kg
412845		Representative	0 - 2 kg
412846		Representative	0 - 2 kg

Table 2. Rock samples

GGU no	Design	Other information	Weight
412847		Representative	0 - 2 kg
412848		Representative	0 - 2 kg
412849		Representative	0 - 2 kg
412850		Representative	0 - 2 kg
412851		Representative	0 - 2 kg
412852		Representative	0 - 2 kg
412853		Representative	0 - 2 kg
412854		Representative	0 - 2 kg
412855		Representative	0 - 2 kg
412856		Representative	0 - 2 kg
412857		Representative	0 - 2 kg
412858		Representative	0 - 2 kg
412859		Representative	0 - 2 kg
412860		Representative	0 - 2 kg
412861		Representative	0 - 2 kg
412862		Representative	0 - 2 kg
412863		Representative	0 - 2 kg
412864		Representative	0 - 2 kg
412865		Representative	0 - 2 kg
412866		Representative	0 - 2 kg
412867		Representative	0 - 2 kg
412868		Representative	0 - 2 kg
412869		Representative	0 - 2 kg
412870		Representative	0 - 2 kg
412871		Representative	0 - 2 kg
412872		Representative	0 - 2 kg
412873		Representative	0 - 2 kg
412874		Representative	0 - 2 kg
412875		Representative	0 - 2 kg
412876		Representative	0 - 2 kg
412877		Representative	0 - 2 kg
412878		Representative	0 - 2 kg
412879		Representative	0 - 2 kg
412880		Representative	0 - 2 kg
412881		Representative	0 - 2 kg
412882		Representative	0 - 2 kg
412883		Representative	0 - 2 kg
412884		Representative	0 - 2 kg
412885		Representative	0 - 2 kg
412886		Representative	0 - 2 kg
412887		Representative	0 - 2 kg
412888		Representative	0 - 2 kg
412889		Loose block	0 - 2 kg
412890		Representative	0 - 2 kg
412891		Representative	0 - 2 kg
412892		Representative	0 - 2 kg
412893		Representative	0 - 2 kg

Table 2. Rock samples

GGU no	Design	Other information	Weight
412894		Representative	0 - 2 kg
412895		Representative	0 - 2 kg
412896		Representative	0 - 2 kg
412897		Representative	0 - 2 kg
412898		Representative	0 - 2 kg
412899		Representative	0 - 2 kg
412901		Representative	0 - 2 kg
412902		Representative	0 - 2 kg
412903		Representative	0 - 2 kg
412904		Representative	0 - 2 kg
412905		Representative	0 - 2 kg
412906		Representative	0 - 2 kg
412907		Representative	0 - 2 kg
412908		Representative	0 - 2 kg
412909		Representative	0 - 2 kg
412910		Representative	0 - 2 kg
412911		Representative	0 - 2 kg
412912		Loose block	0 - 2 kg
412913		Loose block	0 - 2 kg
412914		Loose block	0 - 2 kg
412915		Loose block	0 - 2 kg
412916		Loose block	2 - 5 kg
413001		Ore mineral, loose block	0 - 2 kg
413002		Ore mineral, loose block	0 - 2 kg
413003		Loose block	0 - 2 kg
413004		Loose block	0 - 2 kg
413005		Loose block	0 - 2 kg
413006		Loose block	0 - 2 kg
413007		Loose block	0 - 2 kg
413008		Ore mineral	0 - 2 kg
413009		Ore mineral	0 - 2 kg
413010		Loose block	0 - 2 kg
413011		Ore mineral	0 - 2 kg
413012		Ore mineral, loose block	0 - 2 kg
413013		Ore mineral, loose block	
413014		Loose block	0 - 2 kg
413015		Ore mineral	0 - 2 kg
413016		Ore mineral	0 - 2 kg
413017		Oil mineral, loose block	0 - 2 kg
413018		Ore mineral, loose block	0 - 2 kg
413019		Ore mineral, loose block	0 - 2 kg
413020		Ore mineral, loose block	0 - 2 kg
413021		Ore mineral, loose block	0 - 2 kg
413022			2 - 5 kg
413023			2 - 5 kg
413024			2 - 5 kg
413025		Ore mineral	0 - 2 kg

Table 2. Rock samples

GGU no	Design	Other information	Weight
413026		Ore mineral	0 - 2 kg
413027		Ore mineral	2 - 5 kg
413028			0 - 2 kg
413029			0 - 2 kg

Table 2. Rock samples

GGU no	Origin	Composition
411614	Magmatic, extrusive	mafic, medium-grained
411615	Magmatic, extrusive	mafic, medium-grained
411617	Unknown	mafic, medium-grained
411639	Unknown	heterogeneous, mafic, medium-grained
411645	Unknown	intermediate, fine-grained
411654	Volcanogenic-sedimentary	felsic, fine-grained
412007	Magmatic, plutonic	felsic, medium-grained
412807	Magmatic, plutonic	felsic, coarse-grained
412808	Magmatic, plutonic	felsic, fine-grained
412809	Magmatic, plutonic	felsic, coarse-grained
412810	Magmatic, plutonic	felsic, coarse-grained
412811	Magmatic, plutonic	mafic, fine-grained
412812	Magmatic, plutonic	intermediate, medium-grained
412813	Magmatic, plutonic	felsic, fine-grained
412814	Magmatic, plutonic	felsic, siliceous, fine-grained
412815	Magmatic, plutonic	felsic, siliceous, fine-grained
412816	Magmatic, plutonic	mafic, fine-grained
412817	Magmatic, plutonic	intermediate, medium-grained
412818	Magmatic, plutonic	intermediate, medium-grained
412819	Magmatic, plutonic	felsic, siliceous, fine-grained
412820	Magmatic, plutonic	felsic, siliceous, fine-grained
412821	Magmatic, plutonic	intermediate, medium-grained
412822	Magmatic, plutonic	felsic, siliceous, medium-grained
412823	Magmatic, plutonic	intermediate, medium-grained
412824	Magmatic, plutonic	felsic, siliceous, fine-grained
412825	Magmatic, plutonic	mafic, medium-grained
412826	Magmatic, plutonic	intermediate, medium-grained
412827	Magmatic, plutonic	felsic, siliceous, fine-grained
412828	Volcanogenic-sedimentary	felsic, siliceous, medium-grained
412829	Volcanogenic-sedimentary	intermediate, fine-grained
412830	Magmatic, plutonic	felsic, siliceous, fine-grained
412831	Volcanogenic-sedimentary	intermediate, fine-grained
412832	Magmatic, plutonic	ultramafic, medium-grained
412833	Magmatic, extrusive	mafic, fine-grained
412834	Magmatic, plutonic	ultramafic, medium-grained
412835	Volcanogenic-sedimentary	felsic, siliceous, fine-grained
412836	Volcanogenic-sedimentary	felsic, siliceous, fine-grained
412837	Volcanogenic-sedimentary	felsic, siliceous, medium-grained
412838	Volcanogenic-sedimentary	intermediate, fine-grained
412839	Magmatic, extrusive	mafic, medium-grained
412840	Volcanogenic-sedimentary	felsic, siliceous, fine-grained
412841	Volcanogenic-sedimentary	felsic, siliceous, fine-grained
412842	Volcanogenic-sedimentary	intermediate, medium-grained
412843	Magmatic, extrusive	mafic, medium-grained
412844	Sedimentary	mud
412845	Sedimentary	carbonate, sand
412846	Sedimentary	carbonate, sand

Table 2. Rock samples

GGU no	Origin	Composition
412847	Volcanogenic-sedimentary	felsic, fine-grained
412848	Volcanogenic-sedimentary	felsic, siliceous, fine-grained
412849	Sedimentary	sand, siliceous
412850	Volcanogenic-sedimentary	felsic, siliceous, fine-grained
412851	Magmatic, plutonic	felsic, siliceous, fine-grained
412852	Volcanogenic-sedimentary	felsic, siliceous, fine-grained
412853	Volcanogenic-sedimentary	intermediate, medium-grained
412854	Magmatic, plutonic	felsic, siliceous, fine-grained
412855	Magmatic, plutonic	felsic, siliceous, fine-grained
412856	Magmatic, plutonic	felsic, siliceous, fine-grained
412857	Magmatic, plutonic	intermediate, carbonate, medium-grained
412858	Volcanogenic-sedimentary	intermediate, medium-grained
412859	Volcanogenic-sedimentary	intermediate, medium-grained
412860	Volcanogenic-sedimentary	felsic, fine-grained
412861	Volcanogenic-sedimentary	felsic, siliceous, fine-grained
412862	Magmatic, plutonic	felsic, carbonate, fine-grained
412863	Magmatic, plutonic	felsic, carbonate, fine-grained
412864	Volcanogenic-sedimentary	felsic, siliceous, fine-grained
412865	Sedimentary, carbonate	siliceous
412866	Sedimentary	carbonate
412867	Magmatic, plutonic	felsic, siliceous, fine-grained
412868	Sedimentary	sand
412869	Volcanogenic-sedimentary	felsic, siliceous, fine-grained
412870	Sedimentary	sand
412871	Magmatic	felsic
412872	Volcanogenic-sedimentary	felsic, fine-grained
412873	Volcanogenic-sedimentary	felsic, fine-grained
412874	Magmatic, plutonic	mafic, medium-grained
412875	Magmatic, plutonic	mafic, medium-grained
412876	Magmatic, plutonic	felsic, medium-grained
412877	Sedimentary	conglomerate/breccia
412878	Magmatic, plutonic	intermediate, medium-grained
412879	Sedimentary	sand, siliceous
412880	Volcanogenic-sedimentary	felsic, fine-grained
412881	Magmatic, plutonic	felsic, coarse-grained
412882	Magmatic, extrusive	mafic, fine-grained
412883	Magmatic, plutonic	mafic, medium-grained
412884	Volcanogenic-sedimentary	felsic, siliceous, fine-grained
412885	Volcanogenic-sedimentary	intermediate, heterogeneous,
412886	Magmatic, plutonic	intermediate, medium-grained
412887	Magmatic	mafic
412888	Magmatic, plutonic	felsic, fine-grained
412889	Magmatic, plutonic	intermediate, medium-grained
412890	Magmatic, plutonic	felsic, siliceous, medium-grained
412891	Volcanogenic-sedimentary	intermediate, medium-grained
412892	Volcanogenic-sedimentary	felsic, siliceous, medium-grained
412893	Volcanogenic-sedimentary	intermediate, medium-grained

Table 2. Rock samples

GGU no	Origin	Composition
412894	Volcanogenic-sedimentary	mafic, medium-grained
412895	Volcanogenic-sedimentary	mafic, medium-grained
412896	Volcanogenic-sedimentary	intermediate, medium-grained
412897	Magmatic, extrusive	mafic, fine-grained
412898	Volcanogenic-sedimentary	mafic, medium-grained
412899	Volcanogenic-sedimentary	mafic, medium-grained
412901	Magmatic, plutonic	mafic, medium-grained
412902	Magmatic, extrusive	mafic, medium-grained
412903	Magmatic, plutonic	felsic, siliceous, fine-grained
412904	Volcanogenic-sedimentary	felsic, siliceous, fine-grained
412905	Volcanogenic-sedimentary	felsic, siliceous, fine-grained
412906	Volcanogenic-sedimentary	felsic, siliceous, fine-grained
412907	Volcanogenic-sedimentary	felsic, siliceous, fine-grained
412908	Magmatic, extrusive	mafic, medium-grained
412909	Magmatic, plutonic	mafic, medium-grained
412910	Volcanogenic-sedimentary	felsic, siliceous, fine-grained
412911	Volcanogenic-sedimentary	felsic, siliceous, fine-grained
412912	Magmatic, plutonic	ultramafic, medium-grained
412913	Magmatic, plutonic	ultramafic, medium-grained
412914	Magmatic, plutonic	mafic, medium-grained
412915	Volcanogenic-sedimentary	felsic, fine-grained
412916	Volcanogenic-sedimentary	felsic, medium-grained
413001	Magmatic, plutonic	felsic, coarse-grained
413002	Sedimentary	mud
413003	Magmatic, plutonic	felsic, coarse-grained
413004	Magmatic, plutonic	felsic, fine-grained
413005	Magmatic, plutonic	felsic, fine-grained
413006	Magmatic, plutonic	felsic, fine-grained
413007	Magmatic, plutonic	felsic, medium-grained
413008	Volcanogenic-sedimentary	felsic, siliceous, fine-grained
413009	Magmatic, hypabyssal	felsic, siliceous, medium-grained
413010	Magmatic, hypabyssal	felsic, siliceous, fine-grained
413011	Volcanogenic-sedimentary	felsic, siliceous, fine-grained
413012	Volcanogenic-sedimentary	felsic, siliceous, fine-grained
413013	Volcanogenic-sedimentary	felsic, medium-grained
413014	Magmatic, extrusive	mafic, fine-grained
413015	Volcanogenic-sedimentary	intermediate, fine-grained
413016	Volcanogenic-sedimentary	felsic, fine-grained
413017	Magmatic, hypabyssal	felsic, medium-grained
413018	Volcanogenic-sedimentary	felsic, medium-grained
413019	Volcanogenic-sedimentary	felsic, fine-grained
413020	Volcanogenic-sedimentary	felsic, medium-grained
413021	Volcanogenic-sedimentary	felsic, medium-grained
413022	Magmatic, extrusive	mafic, fine-grained
413023	Magmatic, hypabyssal	felsic, coarse-grained
413024	Magmatic, extrusive	mafic, fine-grained
413025	Volcanogenic-sedimentary	intermediate, fine-grained

Table 2. Rock samples

GGU no	Origin	Composition
413026	Volcanogenic-sedimentary	felsic, fine-grained
413027	Volcanogenic-sedimentary	felsic, siliceous, fine-grained
413028	Sedimentary	carbonate, sand, conglomerate/breccia
413029	Sedimentary	carbonate, sand

Table 2. Rock samples

GGU no	Deformation	Metamorphism	Alteration
411614	Low	High	Unspecified
411615	Low	High	Unspecified
411617	Low	High	Hydrothermal
411639	Low	High	Hydrothermal
411645	Low	High	Hydrothermal
411654	Low	High	Hydrothermal
412007	High	None	Hydrothermal
412807	High	High	None
412808	Low	Low	Unspecified
412809	High	High	Unspecified
412810	High	Low	Hydrothermal
412811	High	High	Unspecified
412812	Low	Low	Unspecified
412813	High	High	Unspecified
412814	Low	Low	Unspecified
412815	Low	Low	Unspecified
412816	Low	Low	Unspecified
412817	High	Low	Hydrothermal
412818	Low	Low	Hydrothermal
412819	None	Low	None
412820	Low	Low	Hydrothermal
412821	Low	Low	Hydrothermal
412822	Low	Low	None
412823	Low	Low	Hydrothermal
412824	Low	Low	Hydrothermal
412825	High	Low	Unspecified
412826	High	Low	Unspecified
412827	High	Low	Hydrothermal
412828	High	Low	Unspecified
412829	High	Low	Unspecified
412830	Low	Low	Hydrothermal
412831	High	Low	Unspecified
412832	None	None	None
412833	None	None	None
412834	None	None	None
412835	High	Low	Unspecified
412836	High	Low	Unspecified
412837	High	Low	Hydrothermal
412838	High	High	Unspecified
412839	High	High	Unspecified
412840	High	High	Unspecified
412841	High	High	Unspecified
412842	High	High	None
412843	High	High	Unspecified
412844	High	High	Unspecified
412845	High	High	None
412846	High	High	None

Table 2. Rock samples

GGU no	Deformation	Metamorphism	Alteration
412847	High	Low	Hydrothermal
412848	High	Low	Unspecified
412849	High	Low	Hydrothermal
412850	High	Low	Hydrothermal
412851	High	Low	None
412852	High	Low	Hydrothermal
412853	High	Low	None
412854	High	Low	Hydrothermal
412855	High	Low	Unspecified
412856	High	Low	Hydrothermal
412857	High	Low	Hydrothermal
412858	High	Low	None
412859	High	Low	None
412860	High	Low	Hydrothermal
412861	High	Low	Hydrothermal
412862	High	Low	Hydrothermal
412863	High	Low	Hydrothermal
412864	High	Low	Hydrothermal
412865	High	High	None
412866	High	High	None
412867	High	High	Hydrothermal
412868	High	High	Unspecified
412869	High	High	Hydrothermal
412870	High	High	Hydrothermal
412871	High	Low	Unspecified
412872	High	High	Hydrothermal
412873	High	High	Hydrothermal
412874	High	High	Hydrothermal
412875	High	High	None
412876	High	High	Hydrothermal
412877	High	High	None
412878	High	High	None
412879	High	High	None
412880	High	High	Hydrothermal
412881	High	High	Unspecified
412882	High	High	None
412883	High	High	None
412884	High	High	Unspecified
412885	Low	Low	None
412886	Low	High	None
412887	High	High	Unspecified
412888	Low	Low	None
412889	Low	Low	Unspecified
412890	High	High	Unspecified
412891	High	High	Hydrothermal
412892	High	High	Hydrothermal
412893	High	High	None

Table 2. Rock samples

GGU no	Deformation	Metamorphism	Alteration
412894	High	High	None
412895	High	High	Hydrothermal
412896	High	High	None
412897	High	High	Hydrothermal
412898	High	High	Hydrothermal
412899	High	High	None
412901	High	High	None
412902	High	High	Hydrothermal
412903	High	Low	None
412904	High	High	Hydrothermal
412905	High	High	Hydrothermal
412906	High	High	Hydrothermal
412907	High	High	Hydrothermal
412908	High	High	None
412909	High	High	None
412910	High	High	Hydrothermal
412911	High	High	Hydrothermal
412912	Low	Low	Hydrothermal
412913	Low	Low	Hydrothermal
412914	Low	Low	Hydrothermal
412915	Low	Low	Hydrothermal
412916	Low	Low	Unspecified
413001	Low	High	Hydrothermal
413002	High	High	None
413003	High	High	None
413004	High	High	None
413005	High	High	None
413006	High	High	None
413007	High	High	None
413008	High	High	None
413009	Low	High	None
413010	Low	High	None
413011	High	High	None
413012	High	High	None
413013	High	High	None
413014	High	Low	Hydrothermal
413015	Low	Low	Hydrothermal
413016	High	High	None
413017	High	High	None
413018	High	High	None
413019	High	High	None
413020	High	High	None
413021	High	High	None
413022	High	High	Hydrothermal
413023	High	Low	None
413024	High	High	Hydrothermal
413025	High	High	Hydrothermal

Table 2. Rock samples

GGU no	Deformation	Metamorphism	Alteration
413026	High	High	None
413027	High	High	None
413028	High	High	Hydrothermal
413029	High	High	None

Table 2. Rock samples

GGU no	Au ppb	Au ppb (fa)	Ag ppm	Ag ppm (icp)	Pt ppb	Pd ppb	Ir ppb	As ppm	Sb ppm	Se ppm	Hg ppm
411614	8		0	0			0	7	1.7	0	0
411615	16		0	0			0	10	2.0	0	0
411617	18		0	1			0	18	1.3	0	0
411639	4		0	2			0	8	0.3	18	0
411645	3		0	0			0	12	0.2	3	0
411654	3		0	0			0	130	0.0	0	0
412007	671/254	600/177	57	46	0	3	0	25	0.4	0	0
412807	0		0	1			0	7	0.0	0	0
412808	0		0	0			0	2	0.0	0	0
412809	5		0	0			0	2	0.3	0	0
412810	239	217	0	0	0	0	0	1	0.4	0	0
412811	2		0	0			0	2	0.6	0	0
412812	15		0	0			0	5	0.7	0	0
412813	25		0	0			0	1	0.0	0	0
412814	23		0	0			0	3	0.6	0	0
412815	0		0	0			0	3	0.3	0	0
412816	14		0	0			0	4	0.9	0	0
412817	13		0	0			0	6	0.3	0	0
412818	18		0	0			0	18	2.0	0	0
412819	8		0	0			0	10	1.5	0	0
412820	5		0	0			0	15	4.0	0	0
412821	4		0	0			0	15	5.5	0	0
412822	2		0	0			0	7	0.8	0	0
412823	7		0	0			0	21	1.8	0	0
412824	0		0	0			0	3	0.5	0	0
412825	37	39	5	0	0	4	0	10	0.4	0	0
412826	4		0	0			0	7	0.3	0	0
412827	5		0	0			0	4	0.2	0	0
412828	0		0	0			0	31	0.6	0	0
412829	7		0	0			0	10	4.6	5	0
412830	0		0	0			0	5	0.2	0	0
412831	5		0	0			0	6	0.8	0	0
412832	0	24	0	3	0	0	0	0	0.2	0	0
412833	4		0	1			0	1	0.2	0	0
412834	0	13	0	2	0	0	0	2	0.0	0	0
412835	12		0	0			0	73	0.4	0	0
412836	9		0	0			0	8	0.0	0	0
412837	29		0	0			0	3	0.7	0	0
412838	30		0	0			0	16	0.3	0	0
412839	9		0	0			0	40	0.3	0	0
412840	33		0	1			0	0	0.0	0	0
412841	18	12	0	0	6	5	0	18	0.0	0	0
412842	28		0	0			0	4	0.2	0	0
412843	6		0	0			0	510	2.1	0	0
412844	27		0	0			0	2	0.2	0	0
412845	0		0	0			0	4	3.2	0	0
412846	9		0	0			0	7	5.1	0	0

Table 2. Rock samples

GGU no	Au ppb	Au ppb	Ag ppm	Ag ppm	Pt ppb	Pd ppb	Ir ppb	As ppm	Sb ppm	Se ppm	Hg ppm
412847	8		0	0			0	8	0.3	0	0
412848	7		0	0			0	4	0.2	0	0
412849	0		0	0			0	11	0.3	0	0
412850	0		0	1			0	2	0.4	0	0
412851	2		0	0			0	1	0.1	0	0
412852	0		0	0			0	3	0.3	0	0
412853	9		0	0			0	3	0.4	0	0
412854	4		0	0			0	4	0.6	0	0
412855	21		0	0			0	3	0.5	0	0
412856	0		0	0			0	36	1.2	0	0
412857	4		0	0			0	11	1.1	0	0
412858	0		0	0			0	28	1.1	0	0
412859	38		0	0			0	2	0.5	0	0
412860	25	30	0	0	5	9	0	6	3.0	0	0
412861	4		0	0			0	5	2.1	0	0
412862	7		0	0			0	9	2.9	0	0
412863	0		0	0			0	21	3.6	0	0
412864	12	15	0	1	0	4	0	220	3.0	0	0
412865	27		0	0			0	11	7.3	0	0
412866	0		0	0			0	2	1.3	0	0
412867	0		0	0			0	1	0.3	0	0
412868	0		0	0			0	1	0.2	0	0
412869	7		0	1			0	0	0.2	0	0
412870	8		0	0			0	0	0.0	0	0
412871	0		0	0			0	1	0.0	0	0
412872	28		0	1			0	8	0.0	0	0
412873	9		0	0			0	6	0.0	0	0
412874	0		0	0			0	4	0.3	0	0
412875	30		0	0			0	2	0.4	0	0
412876	0		0	0			0	2	0.2	0	0
412877	3		0	0			0	3	2.1	0	0
412878	29		0	0			0	2	0.4	0	0
412879	7		0	0			0	0	0.0	0	0
412880	4	2	0	0	11	10	0	52	20.0	0	0
412881	0		0	0			0	22	0.2	0	0
412882	2		0	0			0	3	0.9	0	0
412883	6		0	0			0	2	0.6	0	0
412884	0		0	1			0	13	0.0	0	0
412885	20		0	0			0	2	1.0	0	0
412886	43	29	0	1	0	4	0	6	0.3	0	0
412887	5	32	0	0	0	0	0	4	0.3	0	0
412888	3		0	0			0	0	0.0	0	0
412889	60	22	0	0	0	4	0	1	1.9	0	0
412890	0		0	0			0	4	0.1	0	0
412891	31		0	0			0	8	0.0	0	0
412892	0		0	0			0	3	0.0	0	0
412893	0		0	0			0	6	0.0	0	0

Table 2. Rock samples

GGU no	Au ppb	Au ppb	Ag ppm	Ag ppm	Pt ppb	Pd ppb	Ir ppb	As ppm	Sb ppm	Se ppm	Hg ppm
412894	22		0	0			0	44	0.9	0	0
412895	25	25	0	0	0	4	0	56	0.7	0	0
412896	0		0	0			0	31	0.3	0	0
412897	7		0	0			0	200	1.7	0	0
412898	33		0	0			0	84	1.9	0	0
412899	20		0	0			0	28	1.2	0	0
412901	52	27	0	0	0	0	0	7	2.0	0	0
412902	21		0	0			0	11	1.4	0	0
412903	0		0	0			0	2	0.3	0	0
412904	51	28	0	0	0	0	0	1000	0.0	0	0
412905	7	13	0	0	0	5	0	460	2.8	0	0
412906	6		0	0			0	49	0.9	0	0
412907	40	41	0	1	0	0	0	22	7.7	0	0
412908	18	15	0	0	9	7	0	200	110.0	0	0
412909	0	15	0	0	0	14	0	5	6.3	0	0
412910	13	12	0	0	0	0	0	16	10.0	0	0
412911	7		0	1			0	12	2.0	0	0
412912	2	10	0	0	0	4	0	4	1.8	0	0
412913	49	23	0	0	0	3	0	3	2.2	0	0
412914	15	17	0	0	0	0	0	4	1.4	0	0
412915	2		0	1			0	4	0.3	16	0
412916	12		0	3			0	47	0.3	43	0
413001	33		0	3			0	41	0.4	0	0
413002	8		0	1			0	19	0.5	0	0
413003	0		5	1			0	200	1.1	0	0
413004	2		0	0			0	2	0.2	0	0
413005	0		0	0			0	1	0.2	0	0
413006	0		0	0			0	2	0.2	0	0
413007	0		0	0			0	1	0.3	0	0
413008	2		0	0			0	3	0.2	0	0
413009	0		0	0			0	3	0.1	0	0
413010	0		0	0			0	2	0.2	0	0
413011	0		0	1			0	2	0.3	0	0
413012	0		0	0			0	9	0.3	0	0
413013	0		0	1			0	6	0.0	0	0
413014	0		0	0			0	4	1.0	0	0
413015	81	1	0	2	0	3	0	6	0.9	0	0
413016	7		0	1			0	12	0.3	0	0
413017	0		0	0			0	3	0.3	0	0
413018	2		0	0			0	18	0.3	0	0
413019	28	161	0	1	17	20	0	59	0.5	15	0
413020	34	28	0	1	0	17	0	24	0.8	12	0
413021	65	84	0	1	0	16	0	70	1.1	10	0
413022	10	13	0	0	0	0	0	91	1.6	0	0
413023	3		0	0			0	17	0.9	0	0
413024	4	12	0	0	0	0	0	230	1.4	0	0
413025	6		0	0			0	48	0.6	0	0

Table 2. Rock samples

GGU no	Au ppb	Au ppb	Ag ppm	Ag ppm	Pt ppb	Pd ppb	Ir ppb	As ppm	Sb ppm	Se ppm	Hg ppm
413026	255	179	0	0	0	3	0	17000	4.7	0	0
413027	81	77	0	0	0	0	0	11000	32.0	0	0
413028	3	7	0	1	0	5	0	13	5.2	0	0
413029	0		0	1			0	15	3.3	0	0
Samples	145	32	145	145	32	32	145	145	145	145	145
Minimum	0	1	0	0	0	0	0	0	0.0	0	0
Maximum	671	600	57	46	17	20	0	17000	110.0	43	0

Table 2. Rock samples

GGU no	Cu ppm	Zn ppm	Zn ppm (icp)	Pb ppm	Bi ppm	Mo ppm	Ni ppm	Ni ppm (icp)	Co ppm	Cr ppm	Fe pct
411614	53	270	102	0	0	0	0	153	58	120	11.3
411615	11	0	101	10	0	0	0	104	63	120	6.2
411617	57	486	381	0	0	13	0	40	12	10	15.5
411639	402	914	707	15	6	13	240	303	38	85	23.2
411645	147	500	377	11	0	-	0	82	14	190	7.4
411654	95	433	333	10	0	6	0	71	13	110	6.3
412007	3974	263	251	19	9	17	0	12	8	15	5.7
412807	40	0	8	22	0	0	0	9	0	7	4.6
412808	5	0	16	23	0	0	0	8	2	11	1.2
412809	12	0	18	0	0	0	0	8	6	21	1.6
412810	30	123	65	11	0	0	170	11	52	28	4.8
412811	3	131	116	9	0	0	0	34	26	150	6.2
412812	64	182	93	18	0	0	0	13	46	24	6.8
412813	154	0	43	17	0	0	0	9	28	24	2.4
412814	10	0	14	15	0	0	0	2	24	0	0.7
412815	16	0	9	12	0	0	0	6	2	5	0.7
412816	30	0	73	13	0	0	0	19	36	32	7.0
412817	40	0	22	0	0	0	0	6	3	0	1.8
412818	11	0	34	15	0	0	0	2	38	7	1.7
412819	12	0	16	15	0	-	0	8	1	10	1.0
412820	4	161	149	0	0	0	0	12	13	25	3.9
412821	17	161	114	7	0	0	0	13	15	29	4.2
412822	10	98	65	7	0	0	0	10	9	13	3.7
412823	54	127	96	0	0	0	0	11	17	21	11.5
412824	11	0	50	14	0	0	0	6	6	19	2.0
412825	116	92	88	9	0	4	0	13	11	28	6.2
412826	22	88	129	13	0	0	0	7	10	7	6.0
412827	8	0	2	0	0	2	0	11	0	14	0.3
412828	80	223	210	19	0	3	0	57	13	130	5.9
412829	140	1750	1585	18	0	24	0	148	42	57	14.6
412830	6	0	27	5	0	0	0	7	2	8	0.9
412831	181	1570	1252	20	0	0	240	175	39	98	18.6
412832	98	213	109	0	0	0	190	259	65	260	10.9
412833	32	167	155	0	0	0	70	17	29	15	11.0
412834	80	200	104	0	0	0	440	467	73	440	10.8
412835	170	336	255	19	0	0	0	105	49	120	10.4
412836	103	168	150	10	0	0	0	80	17	150	7.1
412837	26	81	61	18	0	0	120	2	26	120	2.4
412838	6	107	66	25	0	0	0	27	54	66	3.7
412839	10	195	134	27	0	0	130	56	20	130	5.1
412840	29	0	58	11	0	0	0	35	77	51	1.5
412841	44	0	19	8	0	0	0	10	130	7	2.2
412842	20	0	64	36	0	0	160	30	50	86	3.4
412843	37	195	88	7	0	0	0	42	29	140	8.6
412844	1254	0	38	7	0	38	0	7	9	14	3.1
412845	23	128	91	24	0	-	0	30	16	49	4.6
412846	6	141	81	19	0	0	0	31	28	66	4.8

Table 2. Rock samples

GGU no	Cu ppm	Zn ppm	Zn ppm (icp)	Pb ppm	Bi ppm	Mo ppm	Ni ppm	Ni ppm (icp)	Co ppm	Cr ppm	Fe pct
412847	52	228	174	41	0	0	0	28	12	72	4.8
412848	54	0	9	17	0	0	0	16	4	16	1.0
412849	103	278	209	17	0	0	0	61	17	170	4.4
412850	53	0	31	13	0	4	0	20	16	22	4.0
412851	19	0	2	0	0	2	0	13	4	15	0.8
412852	27	0	63	8	0	2	0	35	18	64	5.1
412853	30	162	81	14	0	0	0	56	43	270	7.4
412854	29	81	72	0	0	0	0	37	25	170	5.9
412855	38	84	57	24	0	0	0	5	3	12	2.1
412856	24	58	39	6	0	0	0	28	15	110	3.8
412857	143	0	67	10	0	0	120	106	34	810	5.7
412858	21	101	76	12	0	0	310	221	48	1100	6.7
412859	35	129	72	12	0	0	0	42	36	210	6.7
412860	2	0	4	17	0	33	0	5	1	13	0.4
412861	5	97	53	0	0	1	0	17	3	12	3.3
412862	5	100	80	8	0	3	0	40	24	130	5.1
412863	23	92	66	0	0	0	0	42	26	160	6.2
412864	58	0	42	8	0	0	0	67	27	300	8.2
412865	11	136	91	16	0	0	0	39	30	72	5.1
412866	2	64	37	43	0	0	0	9	6	11	1.1
412867	3	0	2	0	0	3	0	13	0	14	0.4
412868	71	0	52	9	0	0	0	17	12	43	4.1
412869	51	0	27	28	0	0	0	8	2	32	1.9
412870	14	116	78	20	0	0	0	16	5	40	3.2
412871	13	77	69	15	0	0	0	36	22	240	4.7
412872	172	210	151	14	0	29	0	74	13	26	4.6
412873	90	108	50	17	0	24	0	23	7	14	2.6
412874	538	142	115	12	0	0	0	27	41	310	10.4
412875	2	150	131	0	0	0	0	27	52	100	10.9
412876	138	0	11	28	0	-	0	5	1	0	0.9
412877	11	71	71	23	0	0	0	12	4	25	4.1
412878	24	0	102	16	0	0	160	28	25	70	5.8
412879	15	96	69	29	0	0	120	15	40	48	3.1
412880	102	114	92	5	0	0	930	1204	88	1700	9.6
412881	12	104	84	45	0	0	0	12	6	33	3.1
412882	65	188	78	5	0	0	0	115	51	350	9.7
412883	58	154	77	9	0	0	150	122	49	340	9.5
412884	415	213	274	13	0	0	0	159	28	200	7.4
412885	17	158	105	6	0	0	120	24	35	39	8.8
412886	2037	120	54	8	0	0	940	1051	130	460	6.2
412887	2	0	43	7	0	0	0	49	26	220	7.2
412888	11	0	11	0	0	0	0	3	65	23	1.1
412889	73	340	119	0	0	0	0	23	120	0	17.3
412890	38	204	135	8	0	0	0	18	4	69	3.1
412891	7	200	97	8	0	0	0	116	78	300	2.3
412892	58	166	103	23	0	0	0	31	15	72	3.9
412893	7	137	82	16	0	0	0	20	10	52	3.2

Table 2. Rock samples

GGU no	Cu ppm	Zn ppm	Zn ppm (icp)	Pb ppm	Bi ppm	Mo ppm	Ni ppm	Ni ppm (icp)	Co ppm	Cr ppm	Fe pct
412894	55	166	94	10	0	0	0	52	47	200	9.1
412895	31	152	84	11	0	0	0	61	35	420	7.5
412896	21	105	74	18	0	0	0	30	11	72	4.0
412897	59	168	104	7	0	0	0	48	30	190	7.0
412898	46	130	85	7	0	0	120	33	46	56	8.1
412899	9	108	58	9	0	0	0	69	39	110	6.5
412901	39	220	55	6	0	0	0	24	63	30	9.0
412902	33	0	63	0	0	0	0	87	38	130	5.7
412903	3	0	2	5	0	2	0	9	1	11	0.3
412904	117	0	56	10	0	0	0	10	22	18	5.2
412905	99	52	72	10	0	0	0	81	16	70	4.5
412906	80	0	60	10	0	0	0	2	18	0	5.5
412907	135	192	23	8	0	0	510	645	61	1600	8.8
412908	71	107	17	0	0	0	790	1072	76	1500	8.4
412909	62	95	37	0	0	0	660	1036	71	1300	8.8
412910	84	209	119	6	0	3	110	335	19	960	7.6
412911	4	0	32	16	0	6	0	8	0	92	1.6
412912	265	320	159	0	0	0	0	5	120	9	19.1
412913	45	330	153	0	0	0	330	18	97	0	16.1
412914	46	430	130	0	0	0	0	8	100	0	16.9
412915	231	800	487	29	0	51	190	237	13	84	11.9
412916	1373	225	174	22	0	92	540	775	51	130	25.1
413001	334	98	85	44	0	4	130	56	4	53	2.0
413002	131	300	212	0	0	4	96	92	28	110	9.0
413003	68	108	110	15	0	4	0	25	6	37	3.8
413004	23	0	17	6	0	4	0	12	0	27	0.7
413005	15	0	21	22	0	3	0	18	0	27	0.9
413006	9	0	9	5	0	3	0	14	0	17	0.5
413007	12	0	7	51	0	3	0	11	0	17	0.5
413008	54	0	9	0	0	2	0	24	4	10	2.4
413009	12	0	2	0	0	3	25	16	0	24	0.6
413010	7	0	4	0	0	3	0	11	0	9	0.7
413011	17	0	16	0	0	1	22	16	1	19	0.7
413012	211	52	35	0	0	3	0	31	13	68	2.4
413013	19	111	80	18	0	2	0	21	11	42	3.5
413014	9	53	26	5	0	2	0	16	15	90	3.6
413015	974	494	366	0	6	6	0	34	29	130	9.1
413016	94	149	104	18	0	3	0	27	9	62	2.8
413017	53	0	13	9	0	6	0	10	5	13	1.3
413018	119	0	12	11	0	4	0	19	12	4	1.6
413019	545	307	238	14	0	97	320	348	49	82	17.4
413020	634	560	397	13	0	69	320	284	57	90	16.2
413021	663	3110	2400	0	0	89	260	196	50	68	10.5
413022	34	95	61	7	0	0	0	62	36	120	5.7
413023	3	0	30	16	0	0	0	5	2	5	0.7
413024	47	81	60	7	0	0	0	32	19	82	5.3
413025	44	148	95	0	0	3	180	89	41	450	8.2

Table 2. Rock samples

GGU no	Cu ppm	Zn ppm	Zn ppm (icp)	Pb ppm	Bi ppm	Mo ppm	Ni ppm	Ni ppm (icp)	Co ppm	Cr ppm	Fe pct
413026	66	80	51	8	0	3	50	8	14	15	4.1
413027	80	0	51	6	0	0	160	7	17	25	5.2
413028	24	57	59	19	0	5	0	26	7	49	2.3
413029	119	101	67	21	0	4	0	25	7	48	2.7
Samples	145	145	145	145	145	141	145	145	145	145	145
Minimum	2	0	2	0	0	0	0	2	0	0	0.3
Maximum	3974	3110	2400	51	9	97	940	1204	130	1700	25.1

Table 2. Rock samples

GGU no	W ppm	Ta ppm	Sn ppm	Be ppm	Br ppm	Rb ppm	Sc ppm	Cs ppm	Hf ppm	Y ppm	V ppm
411614	-	0	0	0	0.0	0	44.0	0	4	25	304
411615	-	0	0	0	0.0	47	53.0	0	4	26	355
411617	-	0	0	0	0.0	0	1.6	1	0	4	124
411639	5	0	0	0	1.5	44	9.3	3	2	5	147
411645	0	0	0	0	0.0	89	27.0	11	4	7	211
411654	0	0	0	0	0.0	85	26.0	11	2	5	220
412007	180	0	0	0	1.4	60	5.2	0	3	13	42
412807	0	2	0	3	0.0	100	2.6	3	1	7	16
412808	8	0	0	2	0.0	190	1.5	3	4	5	2
412809	6	0	0	0	1.2	15	6.8	2	0	2	30
412810	-	0	0	5	0.0	94	18.0	12	0	10	116
412811	0	0	0	0	0.0	42	23.0	2	2	12	129
412812	-	0	0	0	0.0	61	26.0	4	0	16	139
412813	-	0	0	3	0.0	78	5.1	4	4	4	29
412814	-	0	0	0	0.0	53	1.8	0	0	2	2
412815	0	0	0	0	0.0	25	3.1	2	3	5	11
412816	-	0	0	0	0.0	58	30.0	3	0	11	136
412817	9	0	0	0	0.0	0	7.7	1	3	8	15
412818	-	0	0	0	0.0	0	11.0	0	4	8	29
412819	3	0	0	0	0.0	68	3.2	2	4	8	11
412820	230	0	0	2	0.0	36	15.0	1	3	16	93
412821	12	0	0	0	0.0	0	21.0	0	3	13	87
412822	6	0	0	0	0.0	0	5.4	0	0	7	43
412823	4	1	0	0	0.0	0	11.0	0	2	19	96
412824	0	0	0	0	0.0	160	17.0	11	3	12	81
412825	3	0	0	0	0.0	97	28.0	11	1	11	158
412826	0	0	0	0	0.0	57	18.0	5	3	24	58
412827	8	0	0	0	0.0	0	0.1	0	0	2	2
412828	5	0	0	0	0.0	100	19.0	19	3	7	118
412829	23	0	0	0	0.0	66	11.0	3	1	2	295
412830	8	0	0	0	0.0	67	2.2	13	2	2	2
412831	-	0	0	0	0.0	110	14.0	5	5	5	131
412832	0	7	0	0	0.0	120	21.0	11	9	24	280
412833	0	12	0	0	0.0	99	8.7	2	14	44	55
412834	0	5	0	0	0.0	76	20.0	1	8	20	231
412835	-	0	0	0	0.0	110	34.0	5	3	18	194
412836	6	0	0	0	0.0	23	48.0	1	1	20	300
412837	-	0	0	0	0.0	140	17.0	4	4	4	74
412838	-	0	0	0	0.0	140	13.0	11	5	5	59
412839	-	0	0	0	0.0	150	20.0	17	4	6	101
412840	-	1	0	0	0.0	48	9.0	3	0	4	29
412841	-	1	0	0	0.0	0	0.8	0	0	2	8
412842	-	3	0	0	0.0	71	12.0	6	6	5	59
412843	-	0	0	0	0.0	38	53.0	3	2	17	290
412844	4	0	0	0	0.0	62	7.0	0	10	8	31
412845	0	2	0	0	0.0	150	15.0	8	4	25	79
412846	-	0	0	0	0.0	120	17.0	8	4	16	86

Table 2. Rock samples

GGU no	W ppm	Ta ppm	Sn ppm	Be ppm	Br ppm	Rb ppm	Sc ppm	Cs ppm	Hf ppm	Y ppm	V ppm
412847	7	0	0	0	0.0	270	12.0	3	8	10	68
412848	12	0	0	0	0.0	27	1.1	0	5	2	9
412849	7	0	0	0	0.0	100	18.0	3	4	10	177
412850	4	0	0	0	0.0	0	13.0	1	3	6	48
412851	5	0	0	0	0.8	0	0.6	0	0	2	2
412852	0	1	0	0	0.0	0	17.0	0	3	13	111
412853	-	0	0	0	0.0	0	31.0	0	3	12	160
412854	5	0	0	0	0.0	0	26.0	0	2	12	174
412855	6	0	0	2	0.0	99	4.2	3	6	7	6
412856	0	1	0	0	0.0	0	16.0	0	1	10	102
412857	0	0	0	0	0.0	43	33.0	0	2	14	142
412858	-	0	0	0	0.0	59	31.0	2	2	12	126
412859	-	0	0	0	0.0	49	30.0	0	3	13	165
412860	9	1	0	0	0.0	40	2.0	0	2	5	51
412861	7	0	0	0	0.0	0	1.2	0	0	5	34
412862	9	0	0	0	0.0	0	28.0	3	3	14	154
412863	0	0	0	0	0.0	0	23.0	0	1	10	133
412864	0	0	0	0	0.0	63	46.0	6	3	29	235
412865	-	0	0	0	0.0	98	20.0	10	4	20	94
412866	3	0	0	0	0.7	27	3.6	2	1	11	15
412867	4	0	0	0	0.0	0	0.2	0	0	2	2
412868	7	2	0	0	0.0	0	20.0	0	5	26	53
412869	5	2	0	2	0.0	85	7.6	5	6	10	19
412870	5	0	0	0	2.6	140	7.8	4	6	11	40
412871	0	0	0	0	0.0	65	22.0	2	5	12	122
412872	4	2	0	0	0.0	91	24.0	1	12	36	35
412873	0	0	0	0	0.0	110	20.0	2	10	24	13
412874	2	0	0	0	0.0	43	32.0	2	2	16	208
412875	-	0	0	0	0.0	0	44.0	2	3	24	216
412876	0	2	0	2	0.0	480	1.6	3	11	25	5
412877	2	1	0	0	0.0	92	6.6	0	5	25	23
412878	-	2	0	2	0.0	130	18.0	0	9	28	86
412879	-	0	0	0	0.0	40	6.8	0	5	14	50
412880	0	0	0	0	0.0	55	28.0	15	2	11	174
412881	4	3	0	0	0.0	240	10.0	8	0	13	34
412882	-	0	0	0	0.0	43	49.0	0	2	16	237
412883	-	0	0	0	0.0	15	48.0	0	0	16	227
412884	-	0	0	0	2.1	64	28.0	3	3	20	215
412885	-	0	0	0	0.0	41	19.0	3	4	20	122
412886	-	0	0	0	0.0	53	7.4	1	0	2	35
412887	0	0	0	0	0.0	89	36.0	5	3	29	212
412888	-	0	0	0	0.0	25	5.0	0	5	4	19
412889	-	0	0	0	0.0	0	77.0	0	0	10	1152
412890	6	1	0	0	1.0	0	13.0	0	1	14	167
412891	-	3	0	0	0.0	0	26.0	0	5	24	101
412892	8	0	0	2	0.0	110	19.0	2	6	28	72
412893	7	1	0	0	0.0	160	11.0	8	7	6	60

Table 2. Rock samples

GGU no	W ppm	Ta ppm	Sn ppm	Be ppm	Br ppm	Rb ppm	Sc ppm	Cs ppm	Hf ppm	Y ppm	V ppm
412894	-	0	0	0	0.0	37	33.0	1	3	19	191
412895	8	0	0	0	0.0	37	36.0	6	2	13	166
412896	6	1	0	0	0.0	140	14.0	7	6	7	61
412897	9	0	0	0	0.0	31	30.0	8	3	22	181
412898	-	0	0	0	0.0	0	36.0	2	3	24	169
412899	-	0	0	0	0.0	57	31.0	32	2	17	132
412901	-	0	0	0	0.0	0	53.0	10	3	18	226
412902	-	0	0	0	0.0	0	32.0	0	0	17	142
412903	7	0	0	0	0.0	0	0.2	0	0	2	2
412904	-	0	0	0	0.0	0	12.0	5	3	17	54
412905	5	1	0	2	0.0	47	15.0	4	3	24	91
412906	-	0	0	2	0.0	67	10.0	16	5	18	47
412907	-	1	0	0	0.0	17	26.0	0	2	11	168
412908	-	0	0	0	0.0	0	25.0	0	2	12	158
412909	-	0	0	0	0.0	0	26.0	3	2	12	182
412910	3	1	0	0	0.0	0	20.0	0	2	14	195
412911	4	1	0	2	0.0	72	13.0	3	5	10	68
412912	-	0	0	0	0.0	0	40.0	5	0	8	67
412913	-	0	0	0	0.0	0	62.0	0	0	11	1160
412914	-	0	0	0	0.0	57	58.0	3	0	11	659
412915	10	1	0	0	0.0	72	9.4	5	2	8	745
412916	6	0	0	0	0.0	0	13.0	0	4	28	452
413001	0	0	0	0	0.0	160	9.2	2	4	19	85
413002	4	0	0	0	0.0	0	39.0	0	0	20	232
413003	9	6	0	2	0.0	300	20.0	51	1	2	44
413004	3	0	0	0	2.8	26	2.6	2	0	2	15
413005	6	0	0	0	22.0	15	0.8	3	0	2	6
413006	1	0	0	0	7.5	0	0.3	0	0	2	3
413007	5	4	0	0	0.0	170	4.5	3	2	5	20
413008	0	0	0	0	0.0	0	0.1	0	0	2	4
413009	4	0	0	0	0.0	0	0.1	0	0	2	2
413010	0	0	0	0	0.0	0	0.2	0	0	2	6
413011	5	0	0	0	0.0	0	0.3	0	0	2	5
413012	0	0	0	0	0.0	74	8.0	3	4	6	43
413013	5	2	0	3	0.0	89	9.0	2	4	14	34
413014	0	0	0	0	0.0	0	15.0	1	1	7	107
413015	6	1	0	0	0.0	30	21.0	3	3	24	165
413016	18	8	0	2	0.0	110	3.6	9	7	7	38
413017	0	0	0	2	0.0	30	1.8	0	10	6	2
413018	0	0	0	2	0.0	50	1.7	1	10	7	2
413019	0	1	0	0	0.0	100	8.8	4	2	13	1133
413020	0	0	0	0	0.0	84	14.0	4	3	18	806
413021	7	0	0	0	0.0	18	4.9	1	1	13	421
413022	5	0	0	0	0.0	0	31.0	0	2	18	140
413023	3	4	0	5	0.0	200	3.4	20	0	12	4
413024	2	0	0	0	0.0	17	25.0	3	2	19	124
413025	0	0	0	0	2.0	24	34.0	6	2	18	210

Table 2. Rock samples

GGU no	W ppm	Ta ppm	Sn ppm	Be ppm	Br ppm	Rb ppm	Sc ppm	Cs ppm	Hf ppm	Y ppm	V ppm
413026	0	1	0	0	0.0	0	10.0	6	6	18	47
413027	6	0	0	0	0.0	0	16.0	5	5	19	56
413028	2	0	0	0	0.0	84	8.1	5	5	22	41
413029	9	2	0	2	0.0	170	8.5	22	7	24	53
Samples	99	145	145	145	145	145	145	145	145	145	145
Minimum	0	0	0	0	0.0	0	0.1	0	0	2	2
Maximum	230	12	0	5	22.0	480	77.0	51	14	44	1160

Table 2. Rock samples

GGU no	U ppm	Th ppm	La ppm	Ce ppm	Nd ppm	Sm ppm	Eu ppm	Tb ppm	Yb ppm	Lu ppm	P pct
411614	0.0	0.0	8	24	18	4.9	1.8	1.5	3.70	0.54	0.060
411615	0.0	0.0	9	28	24	5.6	1.8	0.0	4.30	0.58	0.072
411617	1.3	0.0	1	0	0	0.3	0.3	0.0	0.30	0.09	0.005
411639	21.0	5.4	15	26	11	1.8	0.7	0.0	2.50	0.46	0.031
411645	5.2	8.5	25	47	22	4.2	1.1	0.7	2.80	0.42	0.091
411654	11.0	5.2	18	32	15	3.1	1.0	0.0	2.50	0.37	0.055
412007	12.0	9.4	13	31	11	1.8	0.6	0.0	1.70	0.28	0.036
412807	11.0	3.5	4	8	0	1.0	0.4	0.6	1.90	0.27	0.054
412808	6.0	18.0	34	59	23	3.6	0.3	0.0	0.90	0.18	0.007
412809	0.6	1.0	3	7	0	0.7	0.3	0.0	0.50	0.09	0.014
412810	1.4	1.6	7	20	5	2.1	0.6	0.6	1.80	0.26	0.040
412811	1.2	1.1	18	34	16	3.2	1.5	0.0	1.30	0.16	0.123
412812	2.0	7.6	21	44	14	4.6	1.3	1.1	2.50	0.42	0.071
412813	3.1	5.7	21	40	16	2.4	0.9	0.0	0.80	0.13	0.038
412814	3.6	13.0	20	63	14	2.1	0.4	0.0	1.00	0.20	0.006
412815	3.3	13.0	9	47	6	1.0	0.3	0.0	1.00	0.18	0.007
412816	2.1	1.7	12	29	10	3.3	1.1	0.0	2.50	0.36	0.059
412817	4.6	9.3	8	13	0	1.0	0.3	0.0	1.40	0.25	0.022
412818	4.3	5.1	18	44	12	3.0	0.9	0.0	1.80	0.28	0.033
412819	5.5	47.0	4	12	0	1.1	0.3	0.0	1.30	0.18	0.011
412820	5.0	7.1	18	33	14	2.6	0.8	0.6	2.20	0.31	0.060
412821	5.3	6.4	27	47	13	2.9	1.4	0.0	2.30	0.37	0.060
412822	2.5	2.1	12	22	7	1.0	0.4	0.0	0.90	0.15	0.023
412823	3.6	2.7	8	24	19	3.2	1.6	0.0	2.60	0.40	0.057
412824	2.3	5.8	4	11	5	1.2	0.4	0.0	1.60	0.25	0.039
412825	0.0	1.2	10	21	10	2.2	0.9	0.0	1.70	0.27	0.081
412826	3.6	7.2	30	37	12	2.6	1.2	0.0	3.00	0.46	0.053
412827	0.0	0.0	0	0	0	0.0	0.0	0.0	0.00	0.00	0.044
412828	3.9	11.0	29	57	25	4.1	1.1	0.0	2.80	0.41	0.052
412829	37.0	5.8	14	26	9	1.4	0.5	0.0	3.50	0.62	0.006
412830	3.4	5.5	17	33	10	2.8	0.4	0.0	1.90	0.30	0.008
412831	18.0	12.0	32	65	29	4.7	1.2	0.0	2.80	0.48	0.039
412832	2.9	7.2	65	120	51	9.3	3.4	0.8	1.50	0.17	0.275
412833	2.7	6.8	110	200	82	15.0	6.0	2.0	3.60	0.58	0.717
412834	0.0	6.1	54	110	51	10.0	3.6	1.5	1.60	0.19	0.211
412835	6.7	7.3	20	47	17	4.5	1.4	1.1	3.20	0.51	0.035
412836	3.5	0.0	2	4	0	1.9	1.0	0.0	2.90	0.42	0.045
412837	4.0	13.0	37	80	31	5.9	1.1	0.0	2.90	0.43	0.026
412838	4.3	14.0	36	76	32	5.5	1.1	0.0	2.70	0.41	0.044
412839	5.5	12.0	36	78	26	6.0	1.2	0.8	2.80	0.52	0.057
412840	3.0	11.0	30	63	22	4.5	1.0	0.0	2.20	0.30	0.037
412841	2.1	0.6	0	0	0	0.0	0.0	0.0	0.00	0.00	0.004
412842	3.6	14.0	37	81	28	5.9	1.5	0.9	2.90	0.47	0.061
412843	1.8	0.0	2	9	7	2.5	1.1	0.0	3.40	0.50	0.029
412844	5.7	7.4	29	62	24	5.5	1.4	1.4	6.30	0.99	0.029
412845	5.7	12.0	37	69	30	5.1	1.2	1.0	3.00	0.42	0.054
412846	6.0	8.9	26	61	19	4.8	1.1	0.0	2.80	0.42	0.050

Table 2. Rock samples

GGU no	U ppm	Th ppm	La ppm	Ce ppm	Nd ppm	Sm ppm	Eu ppm	Tb ppm	Yb ppm	Lu ppm	P pct
412847	20.0	35.0	62	110	44	8.4	1.2	1.4	1.70	0.29	0.035
412848	33.0	3.4	4	7	0	0.0	0.5	0.0	0.80	0.12	0.009
412849	12.0	8.5	25	48	17	3.9	1.1	0.7	2.60	0.42	0.059
412850	0.0	3.0	17	33	19	3.5	1.2	0.0	1.90	0.32	0.079
412851	0.9	0.5	2	4	0	0.2	0.2	0.0	0.20	0.00	0.006
412852	0.0	1.5	11	21	11	2.4	0.8	0.6	1.70	0.24	0.052
412853	0.0	1.4	14	31	18	3.4	1.2	0.9	2.40	0.35	0.055
412854	0.0	1.9	10	20	0	2.4	0.9	0.0	1.60	0.27	0.056
412855	3.9	15.0	37	73	23	4.3	1.0	0.0	2.10	0.30	0.017
412856	0.6	0.8	7	15	6	1.6	0.6	0.0	1.00	0.17	0.025
412857	3.3	6.4	20	41	22	4.3	1.3	0.6	1.70	0.25	0.089
412858	2.1	5.8	19	47	20	4.8	1.4	0.0	1.70	0.29	0.079
412859	1.6	1.5	12	28	12	3.3	1.3	0.6	2.10	0.34	0.057
412860	12.0	5.4	8	15	10	2.0	0.8	0.0	1.40	0.27	0.006
412861	2.1	0.6	4	7	0	0.4	0.0	0.0	0.50	0.06	0.026
412862	0.0	1.3	13	28	13	3.0	1.2	0.0	1.90	0.24	0.085
412863	0.0	1.0	6	12	8	1.4	0.6	0.0	1.10	0.16	0.034
412864	1.4	1.1	17	39	23	5.6	1.6	0.8	3.10	0.44	0.062
412865	5.2	8.9	29	67	28	5.4	1.1	0.9	3.00	0.49	0.050
412866	2.2	3.4	18	31	11	1.7	0.3	0.6	0.80	0.14	0.016
412867	0.0	0.0	0	0	0	0.0	0.0	0.0	0.00	0.00	0.002
412868	3.2	6.9	9	19	11	3.1	1.1	1.3	3.50	0.54	0.021
412869	7.0	18.0	48	92	36	5.9	0.9	0.9	3.30	0.49	0.026
412870	7.9	16.0	36	69	27	4.9	1.1	0.9	2.30	0.34	0.031
412871	2.0	7.1	27	51	21	3.9	1.1	0.6	1.50	0.24	0.032
412872	6.4	15.0	53	99	45	9.6	1.1	1.6	5.90	0.87	0.026
412873	5.7	13.0	44	88	39	8.1	1.0	1.3	8.20	1.14	0.013
412874	2.4	1.3	9	18	10	2.2	0.7	0.0	1.80	0.28	0.054
412875	2.0	1.6	7	19	9	3.6	1.1	0.0	4.00	0.59	0.047
412876	6.4	36.0	120	200	62	9.1	0.5	1.3	6.20	0.93	0.194
412877	3.7	8.7	35	69	28	4.8	0.9	0.7	3.10	0.48	0.034
412878	2.7	3.2	56	130	58	12.0	2.6	1.2	3.80	0.60	0.133
412879	12.0	2.5	27	56	21	4.2	1.0	0.0	2.40	0.38	0.035
412880	0.0	1.5	7	13	7	2.1	0.8	0.0	1.30	0.19	0.040
412881	13.0	71.0	120	230	90	18.0	0.8	2.8	6.30	0.94	0.025
412882	0.0	0.0	3	13	6	2.3	0.9	0.6	2.50	0.40	0.025
412883	0.0	0.6	3	9	0	2.2	0.9	0.0	2.50	0.43	0.020
412884	11.0	4.3	18	47	13	3.9	1.6	0.8	2.60	0.46	0.054
412885	3.9	5.9	27	71	33	6.8	2.1	0.0	3.30	0.58	0.151
412886	0.0	0.0	1	0	0	0.4	0.3	0.0	0.40	0.07	0.005
412887	1.2	2.3	10	24	12	3.9	1.0	0.9	3.50	0.49	0.042
412888	2.5	8.1	3	6	0	0.7	0.6	0.0	1.00	0.17	0.014
412889	0.0	1.1	3	8	0	1.5	0.9	0.0	1.40	0.30	0.004
412890	6.7	1.3	11	21	13	1.9	0.8	0.0	1.60	0.24	0.108
412891	15.0	2.7	20	48	24	5.1	1.7	1.1	3.20	0.48	0.093
412892	5.9	18.0	49	92	32	5.9	1.3	1.0	13.80	2.13	0.028
412893	7.1	14.0	37	67	26	4.6	1.0	0.7	3.00	0.40	0.038

Table 2. Rock samples

GGU no	U ppm	Th ppm	La ppm	Ce ppm	Nd ppm	Sm ppm	Eu ppm	Tb ppm	Yb ppm	Lu ppm	P pct
412894	0.0	1.8	11	28	17	4.2	1.5	0.9	3.00	0.43	0.082
412895	1.4	2.6	10	23	11	2.7	1.1	0.5	2.30	0.37	0.052
412896	4.6	15.0	41	76	30	5.6	1.4	0.8	3.30	0.51	0.046
412897	2.2	3.0	12	25	11	3.4	1.0	0.0	3.30	0.52	0.039
412898	1.4	0.5	6	18	12	3.4	1.3	0.8	4.10	0.64	0.051
412899	0.0	0.8	2	8	0	1.9	0.9	0.6	2.50	0.41	0.025
412901	0.0	0.9	5	15	15	3.4	1.3	0.0	3.50	0.44	0.033
412902	0.0	0.0	2	7	0	2.0	0.7	0.0	2.70	0.42	0.027
412903	0.0	0.0	0	0	0	0.0	0.0	0.0	0.00	0.00	0.002
412904	4.5	5.3	19	46	13	4.6	1.5	0.0	2.40	0.35	0.107
412905	4.0	7.2	14	29	9	3.1	0.7	0.7	2.40	0.40	0.083
412906	5.6	7.4	21	51	23	5.6	1.7	0.0	2.70	0.41	0.122
412907	0.0	0.8	7	19	5	2.8	1.1	0.0	1.40	0.22	0.040
412908	0.0	1.1	7	20	11	2.9	1.1	0.0	1.40	0.21	0.036
412909	0.0	1.0	7	21	7	2.8	0.9	0.0	1.50	0.23	0.035
412910	5.0	2.3	9	18	9	2.1	0.9	0.0	1.60	0.28	0.034
412911	7.4	18.0	49	90	37	6.2	1.1	1.0	3.70	0.53	0.033
412912	1.8	0.0	7	20	10	1.8	1.1	0.0	1.70	0.25	0.020
412913	0.0	0.0	3	10	0	1.5	0.7	0.0	1.50	0.12	0.010
412914	0.0	1.4	3	0	0	2.0	1.1	0.0	1.80	0.21	0.015
412915	88.0	10.0	31	45	19	3.0	1.2	0.8	5.60	0.99	0.022
412916	38.0	16.0	47	73	32	5.3	1.1	1.0	3.60	0.60	0.022
413001	8.7	42.0	65	130	52	9.4	1.4	1.6	7.30	1.12	0.024
413002	3.4	0.8	3	7	0	1.2	0.7	0.0	2.90	0.45	0.028
413003	13.0	3.0	8	16	8	1.0	0.0	0.6	1.10	0.19	0.103
413004	0.8	1.6	4	8	0	0.5	0.0	0.0	0.50	0.08	0.002
413005	0.0	0.4	0	0	0	0.0	0.0	0.0	0.00	0.00	0.002
413006	0.0	0.0	0	0	0	0.0	0.0	0.0	0.00	0.00	0.002
413007	4.7	7.4	12	25	8	1.9	0.9	0.0	2.40	0.36	0.045
413008	0.0	0.0	0	0	0	0.0	0.0	0.0	0.10	0.00	0.006
413009	0.0	0.0	0	0	0	0.0	0.0	0.0	0.00	0.00	0.002
413010	0.0	0.0	0	0	0	0.0	0.0	0.0	0.10	0.00	0.002
413011	0.0	0.0	0	0	0	0.0	0.0	0.0	0.00	0.00	0.003
413012	4.7	11.0	29	57	25	4.1	0.6	0.6	0.90	0.14	0.010
413013	8.3	10.0	22	45	16	3.3	0.8	0.6	1.70	0.25	0.048
413014	1.4	1.5	5	12	6	1.3	0.6	0.0	1.00	0.16	0.029
413015	4.9	4.9	22	47	23	4.5	2.0	1.0	3.10	0.51	0.157
413016	8.9	15.0	44	85	35	5.8	1.1	0.9	3.60	0.49	0.041
413017	3.2	4.1	30	58	24	5.6	1.8	1.1	4.80	0.77	0.004
413018	3.8	3.9	19	39	18	3.9	1.6	1.3	7.80	1.13	0.002
413019	67.0	9.1	24	34	14	2.2	1.3	0.8	4.80	0.81	0.032
413020	53.0	11.0	31	55	25	4.1	1.0	0.0	2.60	0.49	0.043
413021	35.0	5.2	18	30	12	2.3	0.5	0.0	2.20	0.40	0.009
413022	0.0	0.0	2	8	0	1.6	0.8	0.6	2.50	0.38	0.027
413023	2.8	9.6	10	24	10	2.4	0.3	0.6	4.00	0.58	0.103
413024	1.5	1.7	9	18	8	2.5	1.1	0.5	2.40	0.36	0.054
413025	2.0	1.4	10	23	15	3.1	1.3	0.0	2.30	0.40	0.071

Table 2. Rock samples

GGU no	U ppm	Th ppm	La ppm	Ce ppm	Nd ppm	Sm ppm	Eu ppm	Tb ppm	Yb ppm	Lu ppm	P pct
413026	7.5	6.1	32	68	33	6.2	2.1	0.0	2.90	0.50	0.120
413027	5.2	7.0	28	54	25	4.5	1.4	0.0	3.10	0.61	0.119
413028	4.8	9.9	33	63	26	4.2	0.9	0.6	2.70	0.37	0.038
413029	4.2	19.0	49	94	34	5.7	0.9	0.9	3.70	0.54	0.042
Samples	145	145	145	145	145	145	145	145	145	145	145
Minimum	0.0	0.0	0	0	0	0.0	0.0	0.0	0.00	0.00	0.002
Maximum	88.0	71.0	120	230	90	18.0	6.0	2.8	13.80	2.13	0.717

Table 2. Rock samples

GGU no	Al pct	Ba ppm	Na pct	K pct	Ca pct	Ca pct (icp)	Sr ppm	Sr ppm (icp)	Mg pct	Mn ppm	Ti pct
411614	7.07	0	0.00	0.20	7	6	0	233	4.68	1599	0.98
411615	8.62	360	0.00	0.13	8	6	0	184	3.47	982	1.15
411617	0.33	0	0.00	0.01	13	10	0	53	7.93	1204	0.02
411639	2.94	160	0.64	0.87	0	0	0	36	0.68	442	0.03
411645	6.95	250	1.33	2.55	2	2	0	107	2.75	602	0.43
411654	6.28	270	1.46	2.00	0	1	0	104	1.99	449	0.31
412007	5.51	490	1.38	2.38	0	0	0	156	0.36	355	0.16
412807	6.90	320	2.13	3.96	0	1	0	110	0.01	77	0.05
412808	6.48	290	2.34	3.99	0	0	0	71	0.04	97	0.04
412809	1.51	92	0.42	0.19	1	1	0	58	0.44	209	0.06
412810	5.14	510	0.00	1.25	3	2	0	186	1.86	563	0.29
412811	8.50	310	2.41	1.23	6	5	0	630	3.82	946	0.65
412812	9.46	700	0.00	1.06	5	5	0	448	2.59	979	0.36
412813	7.64	1200	0.00	0.99	3	2	0	754	0.65	317	0.16
412814	4.20	1400	0.00	2.53	0	0	0	88	0.05	77	0.06
412815	5.88	600	2.85	1.72	1	1	0	125	0.13	116	0.06
412816	8.12	450	0.00	0.83	7	5	0	356	2.22	949	0.30
412817	6.28	200	2.75	0.78	3	2	0	173	0.35	287	0.11
412818	7.14	480	0.00	0.54	6	5	0	221	0.38	287	0.14
412819	6.81	930	1.73	3.95	2	1	0	185	0.21	113	0.08
412820	6.86	740	0.04	0.80	16	14	0	87	1.22	1146	0.29
412821	7.35	290	1.03	0.61	13	10	0	302	1.05	624	0.26
412822	2.83	0	0.02	0.02	9	8	0	103	0.75	1105	0.07
412823	4.76	120	0.04	0.07	17	14	0	151	0.92	2495	0.16
412824	6.78	660	2.17	3.49	2	2	0	118	1.06	228	0.20
412825	8.85	770	2.00	1.97	4	5	0	268	2.91	846	0.40
412826	8.97	230	2.67	1.46	5	5	0	235	2.05	1372	0.22
412827	0.51	0	0.13	0.08	0	0	0	9	0.01	51	0.01
412828	7.15	500	1.45	1.54	0	2	0	155	1.88	511	0.24
412829	2.88	370	0.30	1.24	0	0	0	14	0.44	135	0.10
412830	6.31	200	2.95	1.21	0	1	0	120	0.24	218	0.03
412831	4.99	570	0.00	2.39	0	1	0	79	0.76	279	0.08
412832	3.72	1300	0.53	2.14	7	7	0	926	8.22	1226	2.84
412833	7.38	790	3.20	2.62	6	5	1300	1925	2.56	1867	1.56
412834	3.39	670	1.20	1.20	6	6	0	684	8.64	1186	2.34
412835	6.89	400	0.00	1.15	6	3	0	183	2.83	1064	0.43
412836	7.49	0	0.22	0.01	9	8	0	323	5.83	1153	0.64
412837	6.95	720	0.00	2.56	0	0	0	87	1.04	218	0.18
412838	6.53	700	0.00	1.87	0	1	0	99	0.94	328	0.28
412839	9.00	1400	0.00	4.73	0	1	0	92	1.74	458	0.40
412840	4.82	520	0.00	1.26	0	1	0	60	0.64	279	0.05
412841	0.16	0	0.00	0.01	0	0	0	8	0.06	62	0.01
412842	6.15	380	0.00	1.27	0	2	500	281	0.89	259	0.31
412843	6.17	90	0.00	0.27	8	6	0	134	4.46	1213	0.60
412844	6.60	520	1.92	2.36	0	1	0	151	1.07	157	0.17
412845	7.92	820	1.65	4.22	6	5	0	190	2.12	772	0.29
412846	5.84	4900	0.00	2.92	10	8	570	316	2.56	795	0.28

Table 2. Rock samples

GGU no	Al pct	Ba ppm	Na pct	K pct	Ca pct	Ca pct (icp)	Sr ppm	Sr ppm (icp)	Mg pct	Mn ppm	Ti pct
412847	9.15	660	1.85	5.50	0	1	0	121	1.45	215	0.32
412848	2.22	180	0.82	1.17	0	0	0	37	0.04	29	0.02
412849	6.26	630	1.28	2.09	2	2	0	126	1.54	513	0.34
412850	9.34	770	2.12	1.00	3	2	0	247	1.77	393	0.05
412851	1.83	120	0.83	0.06	0	0	0	58	0.02	39	0.01
412852	8.15	210	3.82	0.27	3	3	0	235	2.20	848	0.35
412853	6.57	490	0.00	0.33	5	4	0	305	4.09	1156	0.46
412854	7.54	220	2.07	0.19	5	5	0	339	3.50	1121	0.48
412855	7.75	870	2.59	3.12	2	1	0	271	0.21	309	0.09
412856	4.52	100	1.27	0.14	4	4	0	310	2.03	728	0.30
412857	7.14	530	2.18	0.64	8	6	0	494	5.31	978	0.30
412858	7.14	980	0.00	1.16	6	5	0	460	7.24	997	0.31
412859	7.71	410	0.00	0.18	6	6	0	458	4.18	1118	0.48
412860	2.08	260	0.34	2.01	0	0	0	21	0.02	12	0.07
412861	0.64	0	0.10	0.03	10	7	0	100	3.86	438	0.02
412862	8.18	370	0.99	0.71	9	10	0	394	3.57	840	0.46
412863	5.00	0	0.48	0.15	12	13	0	261	6.91	1371	0.25
412864	7.37	620	0.97	1.79	6	5	0	465	4.40	938	0.66
412865	7.58	1400	0.00	2.28	11	10	0	234	3.46	827	0.32
412866	2.29	210	0.35	0.53	27	27	0	412	1.82	1058	0.07
412867	0.04	0	0.03	0.03	0	0	0	2	0.01	27	0.01
412868	7.54	0	3.25	0.41	3	3	0	234	1.72	515	0.47
412869	7.32	680	1.84	2.59	0	1	0	125	0.75	142	0.04
412870	6.84	630	1.62	2.85	0	1	0	123	0.62	235	0.16
412871	6.75	680	1.82	1.24	3	4	0	290	3.26	836	0.35
412872	6.05	690	1.96	2.75	1	1	0	83	0.13	425	0.16
412873	5.91	630	1.68	3.38	0	1	0	71	0.05	216	0.11
412874	7.02	260	1.29	0.64	9	8	0	252	3.06	1298	0.54
412875	7.13	0	0.00	0.41	9	8	0	308	3.84	1404	0.71
412876	9.37	480	3.42	6.90	0	1	0	69	0.07	126	0.03
412877	6.53	830	2.96	3.28	4	4	0	256	0.46	1042	0.18
412878	8.72	1300	0.00	3.73	4	3	0	416	2.07	822	0.54
412879	6.50	1400	0.00	2.68	0	1	0	189	0.44	190	0.19
412880	4.31	180	0.45	0.82	4	3	0	102	11.88	1222	0.58
412881	8.19	850	1.75	5.32	0	1	0	150	0.71	340	0.21
412882	7.44	230	0.00	0.15	8	6	0	149	5.81	1239	0.51
412883	7.20	120	0.00	0.17	8	6	0	101	5.77	1217	0.50
412884	7.04	430	0.00	1.41	8	6	500	187	5.06	1470	0.58
412885	10.10	740	0.00	0.97	8	7	0	700	2.63	1258	0.48
412886	12.11	0	0.00	0.09	12	8	0	235	3.34	518	0.07
412887	7.41	240	1.90	1.06	7	7	0	197	4.75	952	0.66
412888	4.57	110	0.00	0.54	2	2	0	83	0.33	124	0.12
412889	6.42	70	0.00	0.37	8	6	0	145	4.31	1351	2.00
412890	3.91	140	0.49	0.08	7	6	0	128	2.73	599	0.28
412891	8.26	230	0.00	0.16	12	9	0	201	4.10	480	0.50
412892	7.33	700	1.80	2.20	2	1	0	232	0.98	505	0.25
412893	6.51	680	2.00	2.29	0	1	0	147	0.77	277	0.25

Table 2. Rock samples

GGU no	Al pct	Ba ppm	Na pct	K pct	Ca pct	Ca pct (icp)	Sr ppm	Sr ppm (icp)	Mg pct	Mn ppm	Ti pct
412894	7.64	190	0.00	0.31	11	9	0	655	3.19	1285	0.58
412895	5.36	270	0.47	0.36	8	6	0	300	3.75	1025	0.41
412896	7.19	560	1.15	2.75	2	1	0	96	0.90	301	0.28
412897	6.46	120	0.31	0.27	8	7	0	160	3.98	1212	0.53
412898	8.05	90	0.00	0.32	9	9	0	211	2.88	1247	0.66
412899	9.19	0	0.00	0.52	7	7	0	273	5.15	966	0.41
412901	7.41	350	0.00	0.34	9	6	0	195	4.66	1109	0.60
412902	9.61	80	0.00	0.14	10	10	0	321	3.78	1040	0.44
412903	0.07	0	0.09	0.01	0	0	0	2	0.01	22	0.01
412904	9.25	690	0.00	0.72	4	4	0	651	1.45	449	0.37
412905	8.16	240	1.29	0.99	3	4	0	158	1.94	526	0.38
412906	9.41	680	0.00	1.22	4	3	0	637	1.29	715	0.37
412907	3.50	0	0.00	0.10	7	5	0	163	11.21	1121	0.55
412908	3.16	60	0.00	0.10	5	5	0	191	12.23	1164	0.60
412909	4.47	300	0.00	0.32	6	5	0	118	11.07	1164	0.67
412910	4.14	130	1.02	0.17	9	8	0	340	9.70	1153	0.52
412911	7.44	330	1.48	1.61	1	2	0	138	1.48	366	0.09
412912	6.11	70	0.00	0.31	7	5	0	120	3.71	2374	1.58
412913	6.52	60	0.00	0.29	8	7	0	182	4.25	1536	2.13
412914	7.13	70	0.00	0.20	9	6	0	192	3.68	1516	1.93
412915	3.85	380	0.66	1.98	0	0	0	84	0.70	173	0.16
412916	2.04	71	0.00	0.01	1	1	0	108	1.29	463	0.34
413001	8.74	1300	1.84	6.07	0	1	0	178	0.73	373	0.22
413002	6.37	200	0.78	0.31	11	9	0	273	4.21	1209	0.36
413003	6.50	100	1.83	3.11	0	0	0	24	0.49	699	0.18
413004	1.43	120	0.26	0.61	0	0	0	25	0.08	49	0.01
413005	0.49	110	0.10	0.24	0	0	0	16	0.04	315	0.01
413006	0.09	0	0.03	0.04	0	0	0	5	0.01	66	0.01
413007	6.70	570	1.31	4.63	0	1	0	117	0.03	38	0.01
413008	0.03	0	0.01	0.01	0	0	0	3	0.33	186	0.01
413009	0.02	0	0.01	0.01	0	0	0	2	0.01	30	0.01
413010	0.16	0	0.02	0.02	0	0	0	2	0.06	37	0.01
413011	0.16	0	0.03	0.01	0	0	0	8	0.04	71	0.01
413012	4.63	130	0.26	0.75	3	2	0	67	0.99	200	0.12
413013	7.42	410	2.98	1.74	3	3	0	245	0.80	380	0.19
413014	4.97	0	0.29	0.52	7	6	0	244	1.24	715	0.27
413015	7.04	130	2.21	0.45	5	5	0	586	4.44	3856	0.49
413016	6.79	650	1.66	2.56	0	1	0	119	0.77	344	0.08
413017	6.31	630	4.15	1.15	0	1	0	118	0.05	65	0.06
413018	6.41	1200	3.52	2.61	0	1	0	152	0.03	70	0.05
413019	3.59	310	0.61	3.20	0	0	0	42	0.47	177	0.17
413020	4.51	210	1.38	1.16	2	1	0	122	1.00	243	0.21
413021	0.64	70	0.08	0.49	0	0	0	7	0.17	60	0.07
413022	9.32	0	1.29	0.14	11	10	0	659	3.15	923	0.45
413023	6.18	190	3.13	2.89	2	1	0	99	0.13	193	0.07
413024	9.58	290	2.03	0.52	9	8	0	613	2.40	823	0.41
413025	7.11	220	0.69	0.39	12	10	0	397	3.52	1419	0.55

Table 2. Rock samples

GGU no	Al pct	Ba ppm	Na pct	K pct	Ca pct	Ca pct (icp)	Sr ppm	Sr ppm (icp)	Mg pct	Mn ppm	Ti pct
413026	8.62	700	3.73	0.62	3	4	640	691	1.29	377	0.36
413027	9.53	600	4.41	0.44	5	4	0	710	1.57	438	0.37
413028	5.58	730	1.90	2.30	5	5	0	165	0.75	867	0.19
413029	7.11	1000	2.33	4.28	1	2	0	150	0.93	533	0.23
Samples	145	145	145	145	145	145	145	145	145	145	145
Minimum	0.0	0	0.00	0.01	0	0	0	2	0.01	12	0.01
Maximum	12.1	4900	4.41	6.90	27	27	1300	1925	12.23	3856	2.84

Table 3. Stream sediment samples and heavy mineral concentrates

GGU no	Altitude metre	-1.0 mm fract. litre	Preconc. gramme	Conc. gramme	Analysis gramme
388151	2				8.4
388152	50				7.7
388153	25				7.9
388154	50				6.6
388155	50				7.2
388156	5				8.6
388157	50				5.9
388158	50				6.4
388159	20				8.9
388160	10				8.5
390751	2	2.0	57.7	43.4	29.1
390752	50	3.0	59.0	43.4	29.2
390753	25	3.0	54.0	42.6	29.7
390754	50	2.0	44.6	24.5	19.2
390755	50	3.0	29.0	8.9	5.6
390756	5	4.0	68.1	37.0	27.7
390757	50	1.5	27.8	8.1	20.3
390758	50	2.0	46.0	20.0	6.0
390759	20	4.0	35.4	28.0	14.6
390760	10	2.5	39.1	15.0	11.3

Notes: 388151-160 are stream sediment samples. The -0.1 mm (-150 mesh) fraction is analysed.
390751-760 are heavy mineral concentrates.

Table 3. Stream sediment samples and heavy mineral concentrates

GGU no	Au ppb	Au ppb (fa)	Ag ppm	Ag ppm (icp)	Pt ppb	Pd ppb	Ir ppb	As ppm	Sb ppm	Se ppm	Hg ppm
388151	8		0	0			0	6	1.9	0	0
388152	3		0	0			0	55	0.3	0	0
388153	39		0	1			0	40	0.0	0	0
388154	0		0	0			0	5	3.2	0	0
388155	4		0	1			0	13	0.6	0	0
388156	0		0	0			0	5	0.4	0	0
388157	0		0	1			0	10	0.7	0	0
388158	6		0	0			0	21	0.9	0	0
388159	0		0	0			0	14	0.4	0	0
388160	0		0	0			0	24	4.2	0	0
Samples	10		10	10			10	10	10	10	10
Minimum	0		0	0			0	5	0.0	0	0
Maximum	39		0	1			0	55	4.2	0	0
390751	18		0	0			0	20	3.7	0	0
390752	253		0	0			0	1100	0.7	0	0
390753	19		0	0			0	1400	0.0	0	0
390754	0		0	0			0	9	5.7	0	0
390755	0		0	0			0	65	0.0	0	0
390756	7		0	0			0	22	0.9	0	0
390757	0		0	0			0	12	0.0	0	0
390758	0		0	0			0	0	0.9	0	0
390759	116		0	0			0	600	0.5	0	0
390760	0		0	0			0	160	5.1	0	0
Samples	10		10	10			10	10	10	10	10
Minimum	0		0	0			0	0	0.0	0	0
Maximum	253		0	0			0	1400	5.7	0	0

Table 3. Stream sediment samples and heavy mineral concentrates

GGU no	Cu ppm	Zn ppm	Zn ppm (icp)	Pb ppm	Bi ppm	Mo ppm	Ni ppm	Ni ppm (icp)	Co ppm	Cr ppm	Fe pct
388151	11	69	41	7	0	0	0	22	8	66	3.0
388152	40	0	64	19	0	0	0	33	10	71	3.5
388153	48	140	86	28	0	0	0	58	19	180	5.4
388154	26	0	93	17	0	-	0	37	16	77	3.9
388155	81	230	189	18	0	28	0	29	19	91	5.7
388156	11	90	41	20	0	-	0	12	7	53	4.0
388157	43	69	109	28	0	-	0	45	16	170	4.0
388158	64	0	113	20	0	-	0	41	19	130	4.6
388159	85	0	87	0	0	0	110	75	32	200	6.1
388160	35	0	77	13	0	-	0	54	12	200	4.4
Samples	10	10	10	10	10	5	10	10	10	10	10
Minimum	11	0	41	0	0	0	0	12	7	53	3.0
Maximum	85	230	189	28	0	28	110	75	32	200	6.1
390751	27	283	36	12		-	0	19	37	790	57.2
390752	50	357	28	12		0	0	49	71	570	60.2
390753	154	850	45	6		0	0	108	110	800	46.3
390754	5	305	25	6		-	0	13	40	490	30.1
390755	38	860	122	8		-	0	14	40	410	23.7
390756	26	505	51	10		-	510	40	49	360	56.6
390757	32	420	67	4		-	0	27	61	930	19.3
390758	10	320	34	6		-	0	15	49	1000	21.8
390759	147	357	12	10		-	0	59	100	430	25.6
390760	15	200	28	6		0	0	28	46	1500	22.5
Samples	10	10	10	10		3	10	10	10	10	10
Minimum	5	200	12	4		0	0	13	37	360	19.3
Maximum	154	860	122	12		0	510	108	110	1500	60.2

Table 3. Stream sediment samples and heavy mineral concentrates

GGU no	W ppm	Ta ppm	Sn ppm	Be ppm	Br ppm	Rb ppm	Sc ppm	Cs ppm	Hf ppm	Y ppm	V ppm
388151	0	1	0	2	0.0	79	14.0	3	6	34	55
388152	4	1	0	0	0.0	72	14.0	8	5	10	74
388153	6	0	0	0	0.0	65	14.0	7	11	19	114
388154	5	0	0	2	12.0	97	18.0	14	6	36	78
388155	0	2	0	0	27.0	110	28.0	0	32	67	97
388156	0	0	0	2	2.4	110	9.2	4	16	25	42
388157	16	0	0	0	31.0	74	15.0	7	19	37	77
388158	0	0	0	2	8.5	140	20.0	18	7	26	105
388159	0	0	0	0	0.0	0	31.0	0	10	23	145
388160	0	0	0	2	3.9	56	15.0	5	10	40	93
Samples	10	10	10	10	10	10	10	10	10	10	10
Minimum	0	0	0	0	0.0	0	9.2	0	5	10	42
Maximum	16	2	0	2	31.0	140	31.0	18	32	67	145
390751	95	20			21.0	0	37.0	0	13		
390752	150	13			280.0	61	14.0	0	12		
390753	270	20			890.0	100	26.0	0	17		
390754	81	8			100.0	0	42.0	0	9		
390755	210	0			820.0	0	230.0	0	31		
390756	0	16			310.0	0	49.0	0	18		
390757	160	0			310.0	95	85.0	0	12		
390758	280	0			440.0	0	40.0	0	29		
390759	130	6			120.0	0	64.0	0	11		
390760	95	2			49.0	54	34.0	0	15		
Samples	10	10			10	10	10	10	10		
Minimum	0	0			21.0	0	14.0	0	9		
Maximum	280	20			890.0	100	230.0	0	31		

Table 3. Stream sediment samples and heavy mineral concentrates

GGU no	U ppm	Th ppm	La ppm	Ce ppm	Nd ppm	Sm ppm	Eu ppm	Tb ppm	Yb ppm	Lu ppm	P pct
388151	3.7	11.0	35	58	18	5.4	1.0	1.0	3.80	0.65	0.085
388152	3.9	12.0	38	60	24	5.5	1.1	0.0	2.40	0.38	0.086
388153	6.0	22.0	78	120	40	11.0	1.9	1.1	3.90	0.66	0.172
388154	13.0	10.0	36	58	24	5.7	1.2	0.0	3.30	0.46	0.078
388155	36.0	43.0	160	250	110	27.0	2.0	3.7	10.50	1.65	0.115
388156	7.0	28.0	87	140	57	12.0	1.3	2.3	5.30	0.81	0.107
388157	50.0	48.0	120	190	71	16.0	1.5	2.3	4.90	0.81	0.159
388158	19.0	12.0	39	66	21	6.0	1.1	0.0	3.90	0.68	0.098
388159	4.0	7.8	25	43	22	4.9	0.8	1.1	3.40	0.48	0.051
388160	7.7	13.0	44	71	31	7.3	1.3	0.0	3.90	0.55	0.128
Samples	10	10	10	10	10	10	10	10	10	10	10
Minimum	3.7	7.8	25	43	18	4.9	0.8	0.0	2.40	0.38	0.051
Maximum	50.0	48.0	160	250	110	27.0	2.0	3.7	10.50	1.65	0.172
390751	42.0	51.0	88	190	46	12.0	1.8	3.0	15.80	2.70	
390752	10.0	8.6	23	48	0	3.1	0.0	0.0	6.80	1.30	
390753	0.0	10.0	32	74	20	5.6	1.8	0.0	3.50	0.60	
390754	35.0	25.0	56	130	52	12.0	2.2	3.0	11.30	2.10	
390755	45.0	190.0	620	1100	450	94.0	0.0	21.0	123.00	16.90	
390756	29.0	140.0	260	520	170	36.0	2.3	0.0	21.90	4.00	
390757	53.0	250.0	620	1100	440	76.0	3.1	15.0	77.70	10.60	
390758	35.0	130.0	260	440	160	34.0	3.2	10.0	42.90	5.80	
390759	25.0	31.0	41	99	44	7.9	1.5	0.0	14.30	2.40	
390760	8.8	23.0	60	120	50	11.0	1.6	0.0	10.00	1.30	
Samples	10	10	10	10	10	10	10	10	10	10	
Minimum	0.0	8.6	23	48	0	3.1	0.0	0.0	3.50	0.60	
Maximum	53.0	250.0	620	1100	450	94.0	3.2	21.0	123.00	16.90	

Table 3. Stream sediment samples and heavy mineral concentrates

GGU no	Al pct	Ba ppm	Na pct	K pct	Ca pct	Ca pct (icp)	Sr ppm	Sr ppm (icp)	Mg pct	Mn ppm	Ti pct
388151	7.06	630	2.28	2.57	3	3	0	253	1.25	501	0.27
388152	7.19	330	2.01	1.65	0	2	0	164	1.14	451	0.30
388153	6.89	510	2.13	1.78	3	2	0	232	1.57	633	0.88
388154	7.95	530	1.82	2.71	4	4	0	268	2.57	830	0.40
388155	7.16	630	2.60	1.97	0	2	0	170	1.17	918	0.30
388156	7.08	680	2.59	3.02	2	2	0	215	0.71	399	0.18
388157	7.41	470	1.91	1.82	3	3	0	315	2.12	792	0.55
388158	7.86	360	1.86	2.44	2	3	0	226	2.13	798	0.45
388159	7.69	210	1.49	0.66	6	6	0	217	4.56	1101	0.63
388160	6.62	600	2.11	2.37	3	4	0	322	1.88	878	0.38
Samples	10	10	10	10	10	10	10	10	10	10	10
Minimum	6.6	210	1.49	0.66	0	2	0	164	0.71	399	0.18
Maximum	8.0	680	2.60	3.02	6	6	0	322	4.56	1101	0.88
390751		450	0.26		0		0			252	
390752		0	0.20		2		0			164	
390753		0	0.23		0		0			468	
390754		0	0.49		15		0			158	
390755		0	0.34		12		0			280	
390756		0	0.15		0		0			432	
390757		0	0.39		10		0			300	
390758		0	0.46		10		0			236	
390759		0	0.70		7		0			58	
390760		0	0.33		8		0			240	
Samples		10	10		10		10			10	
Minimum		0	0.15		0		0			58	
Maximum		450	0.70		15		0			468	

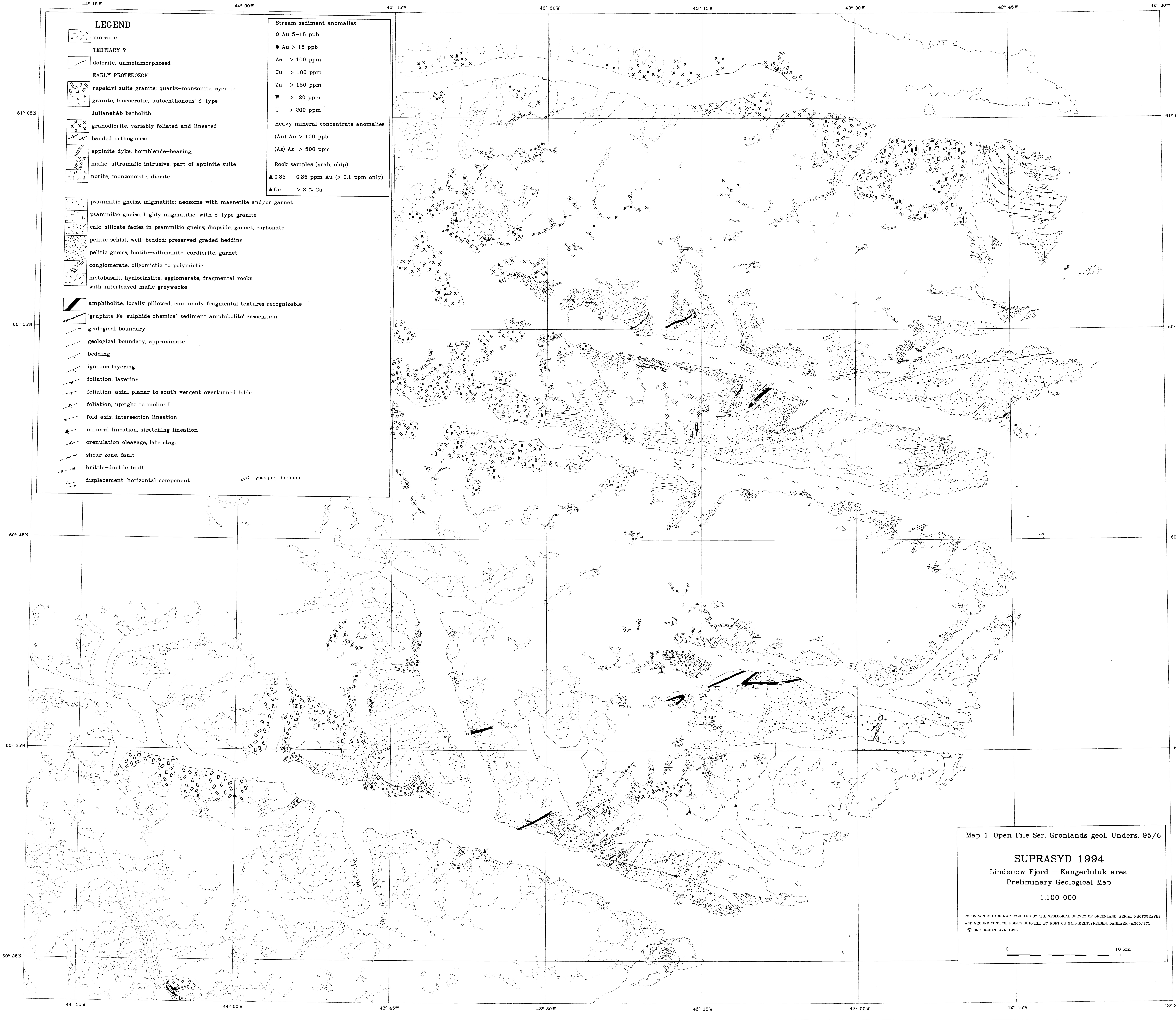
LEGEND
moraine
TERTIARY ?
dolerite, unmetamorphosed
EARLY PROTEROZOIC
rapakivi suite granite; quartz-monzonite, syenite
granite, leucocratic, 'autochthonous' S-type
Julianehåb batholith:
granodiorite, variably foliated and lineated
banded orthogneiss
appinite dyke, hornblende-bearing,
mafic-ultramafic intrusive, part of appinite suite
norite, monzonorite, diorite
psammitic gneiss, migmatitic; neosome with magnetite and/or garnet
psammitic gneiss, highly migmatitic, with S-type granite
calc-silicate facies in psammitic gneiss; diopside, garnet, carbonate
pelitic schist, well-bedded; preserved graded bedding
pelitic gneiss; biotite-sillimanite, cordierite, garnet
conglomerate, oligomictic to polymictic
metabasalt, hyaloclastite, agglomerate, fragmental rocks with interleaved mafic greywacke
amphibolite, locally pillowed, commonly fragmental textures recognizable
'graphite Fe-sulphide chemical sediment amphibolite' association
geological boundary
geological boundary, approximate
bedding
igneous layering
foliation, layering
foliation, axial planar to south vergent overturned folds
foliation, upright to inclined
fold axis, intersection lineation
mineral lineation, stretching lineation
crenulation cleavage, late stage
shear zone, fault
brittle-ductile fault
displacement, horizontal component
younging direction
Stream sediment anomalies
O Au 5-18 ppb
● Au > 18 ppb
As > 100 ppm
Cu > 100 ppm
Zn > 150 ppm
W > 20 ppm
U > 200 ppm
Heavy mineral concentrate anomalies
(Au) Au > 100 ppb
(As) As > 500 ppm
Rock samples (grab, chip)
▲0.35 0.35 ppm Au (> 0.1 ppm only)
▲Cu > 2 % Cu
44° 15'W
44° 00'W
43° 45'W
43° 30'W
43° 15'W
43° 00'W
42° 45'W
42° 30'W
61° 05'N
60° 55'N
60° 45'N
60° 35'N
60° 25'N
Map 1. Open File Ser. Grønlands geol. Unders. 95/6
SUPRASYD 1994
Lindenow Fjord – Kangerluluk area
Preliminary Geological Map
1:100 000
TOPOGRAPHIC BASE MAP COMPILED BY THE GEOLOGICAL SURVEY OF GREENLAND. AERIAL PHOTOGRAPHS AND GROUND CONTROL POINTS SUPPLIED BY KORT OG MATRIKELSTYRELSEN. DANMARK (A.200/87).
© GGU. KØBENHAVN 1995.
0
10 km

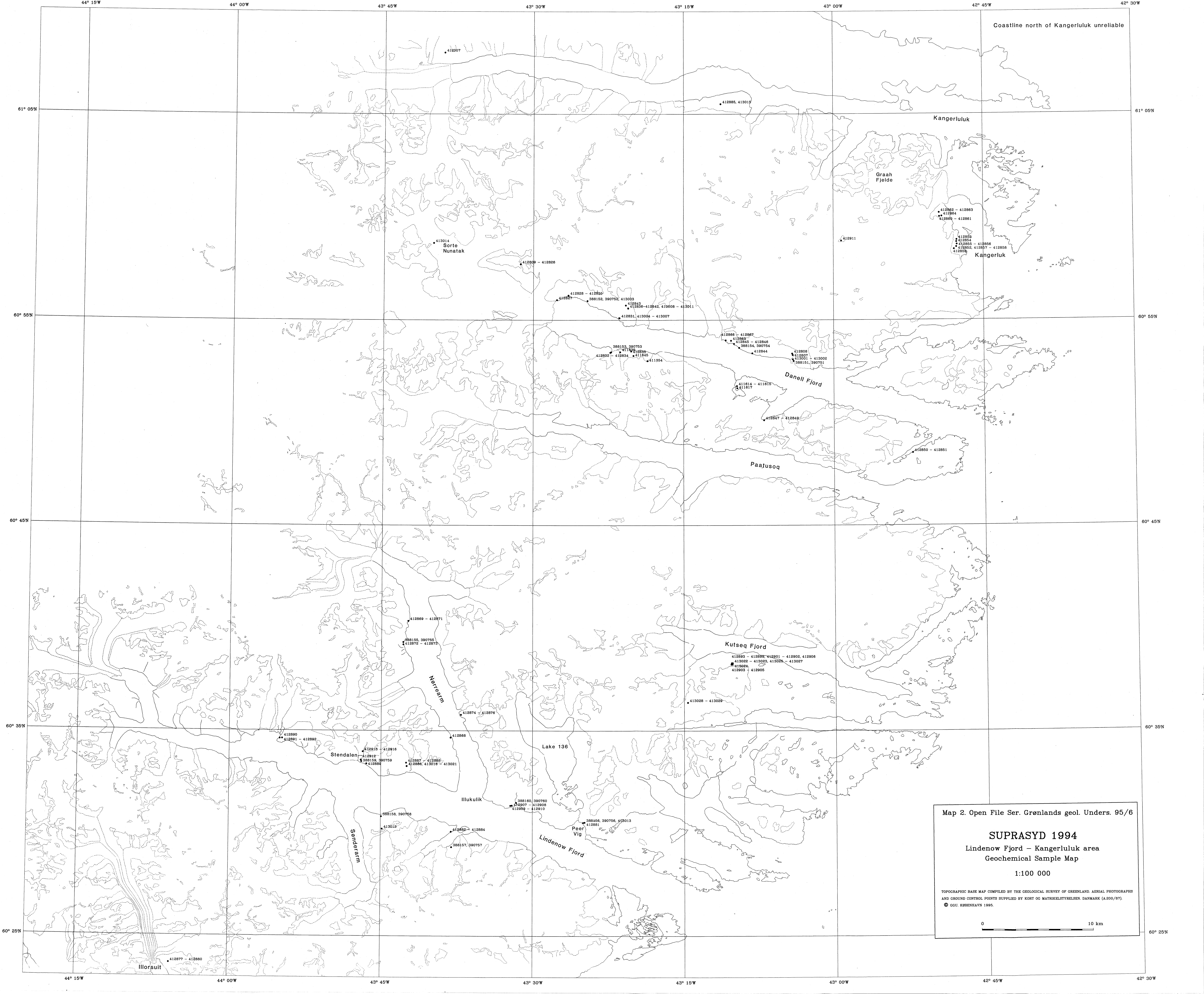

Coastline north of Kangerluluk unreliable
44° 15'W
44° 00'W
43° 45'W
43° 30'W
43° 15'W
43° 00'W
42° 45'W
42° 30'W
61° 05'N
60° 55'N
60° 45'N
60° 35'N
60° 25'N
Kangerluluk
Graah Fjelde
Kangerluk
Sorte Nunatak
Danell Fjord
Paatusoq
Kutseq Fjord
Nørrearm
Lake 136
Stendalen
Illukulik
Peer Vig
Lindenow Fjord
Sønderarm
Illorsuit
Map 2. Open File Ser. Grønlands geol. Unders. 95/6
SUPRASYD 1994
Lindenow Fjord – Kangerluluk area
Geochemical Sample Map
1:100 000
TOPOGRAPHIC BASE MAP COMPILED BY THE GEOLOGICAL SURVEY OF GREENLAND. AERIAL PHOTOGRAPHS AND GROUND CONTROL POINTS SUPPLIED BY KORT OG MATRIKELSTYRELSEN. DANMARK (A.200/87).
© GGU. KØBENHAVN 1995.
0
10 km

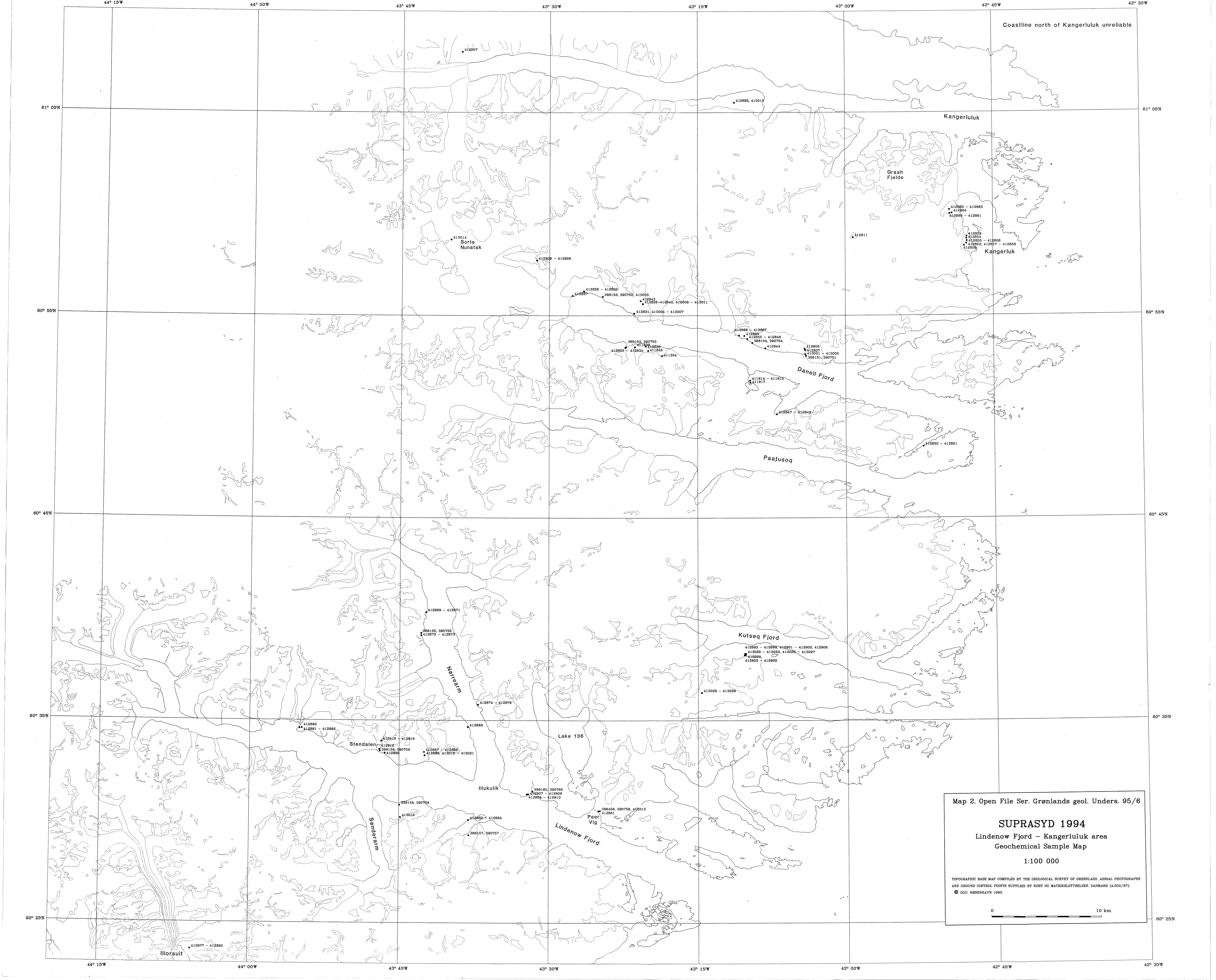
Map 2. Open File Ser. Grønlands geol. Unders. 95/6
SUPRASYD 1994
Lindenow Fjord – Kangerluluk area
Geochemical Sample Map
1:100 000
TOPOGRAPHIC BASE MAP COMPILED BY THE GEOLOGICAL SURVEY OF GREENLAND. AERIAL PHOTOGRAPHS AND GROUND CONTROL POINTS SUPPLIED BY KORT OG MATRIKELSTYRELSEN. DANMARK (A.200/87).
© GGU. KØBENHAVN 1995.
0
10 km
Coastline north of Kangerluluk unreliable
Kangerluluk
Graah Fjelde
Kangerluk
Sorte Nunatak
Danell Fjord
Paatusoq
Kutseq Fjord
Nørrearm
Stendalen
Lake 136
Illukulik
Peer Vig
Lindenow Fjord
Sønderarm
Illorsuit
44° 15'W
44° 00'W
43° 45'W
43° 30'W
43° 15'W
43° 00'W
42° 45'W
42° 30'W
61° 05'N
60° 55'N
60° 45'N
60° 35'N
60° 25'N

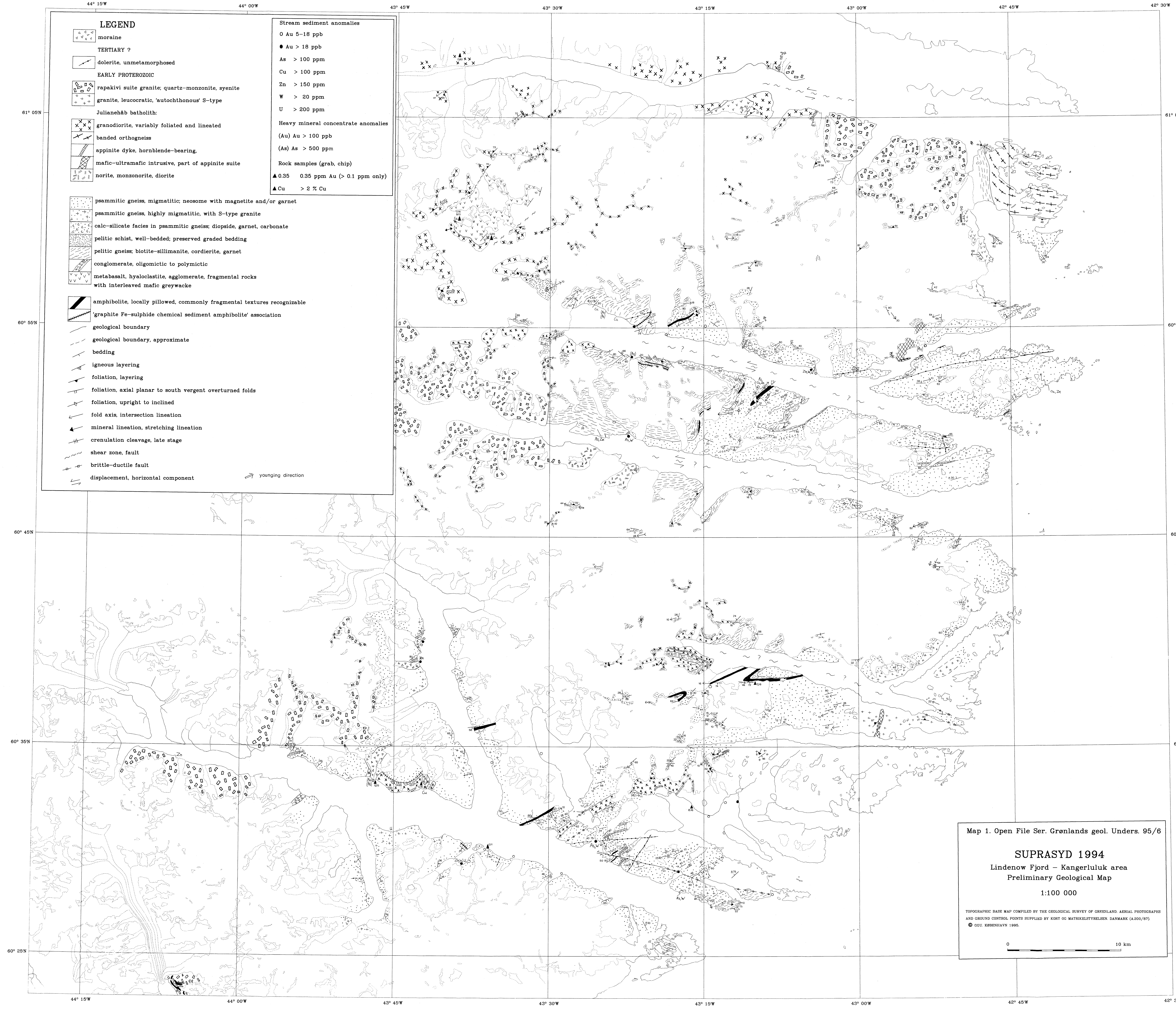

44° 15'W
44° 00'W
43° 45'W
43° 30'W
43° 15'W
43° 00'W
42° 45'W
42° 30'W
61° 05'N
60° 55'N
60° 45'N
60° 35'N
60° 25'N
LEGEND
moraine
TERTIARY ?
dolerite, unmetamorphosed
EARLY PROTEROZOIC
rapakivi suite granite; quartz–monzonite, syenite
granite, leucocratic, 'autochthonous' S–type
Julianehåb batholith:
granodiorite, variably foliated and lineated
banded orthogneiss
appinite dyke, hornblende–bearing,
mafic–ultramafic intrusive, part of appinite suite
norite, monzonorite, diorite
psammitic gneiss, migmatitic; neosome with magnetite and/or garnet
psammitic gneiss, highly migmatitic, with S–type granite
calc–silicate facies in psammitic gneiss; diopside, garnet, carbonate
pelitic schist, well–bedded; preserved graded bedding
pelitic gneiss; biotite–sillimanite, cordierite, garnet
conglomerate, oligomictic to polymictic
metabasalt, hyaloclastite, agglomerate, fragmental rocks with interleaved mafic greywacke
amphibolite, locally pillowed, commonly fragmental textures recognizable
'graphite Fe–sulphide chemical sediment amphibolite' association
geological boundary
geological boundary, approximate
bedding
igneous layering
foliation, layering
foliation, axial planar to south vergent overturned folds
foliation, upright to inclined
fold axis, intersection lineation
mineral lineation, stretching lineation
crenulation cleavage, late stage
shear zone, fault
brittle–ductile fault
displacement, horizontal component
younging direction
Stream sediment anomalies
O Au 5–18 ppb
● Au > 18 ppb
As > 100 ppm
Cu > 100 ppm
Zn > 150 ppm
W > 20 ppm
U > 200 ppm
Heavy mineral concentrate anomalies
(Au) Au > 100 ppb
(As) As > 500 ppm
Rock samples (grab, chip)
▲0.35 0.35 ppm Au (> 0.1 ppm only)
▲Cu > 2 % Cu
Map 1. Open File Ser. Grønlands geol. Unders. 95/6
SUPRASYD 1994
Lindenow Fjord – Kangerluluk area
Preliminary Geological Map
1:100 000
TOPOGRAPHIC BASE MAP COMPILED BY THE GEOLOGICAL SURVEY OF GREENLAND. AERIAL PHOTOGRAPHS AND GROUND CONTROL POINTS SUPPLIED BY KORT OG MATRIKELSTYRELSEN. DANMARK (A.200/87).
© GGU. KØBENHAVN 1995.
0
10 km

ISSN 0903-7322